

UNIVERSITI
TEKNOLOGI
PETRONAS

Wave Attenuation Characteristics of Sand Container

by

Khalid bin Zaid

submitted in partial fulfilment of
the requirements for the
Bachelor of Engineering
(Civil Engineering)

JULY 2007

Universiti Teknologi PETRONAS
Bandar Seri Iskandar
31750 Tronoh
Perak Darul Ridzuan

CERTIFICATION OF APPROVAL

Wave Attenuation Characteristics of a Sand Container

by

Khalid bin Zaid

A project dissertation submitted to the
Civil Engineering Programme
Universiti Teknologi PETRONAS
in partial fulfillment of the requirement for the
BACHELOR OF ENGINEERING (Hons)
(CIVIL ENGINEERING)

Approved by,

(Mr Teh Hee Min)

UNIVERSITI TEKNOLOGI PETRONAS
TRONOH, PERAK
December 2007

CERTIFICATION OF ORIGINALITY

This is to certify that I am responsible for the work submitted in this project, that the original work is my own except as specified in the references and acknowledgements, and that the original work contained herein have not been undertaken or done by unspecified sources or persons.

KHALID BIN ZAID

ACKNOWLEDGEMENT

I would like to express my deepest gratitude to individuals who have collaborated and assisted me directly or indirectly throughout the semester in completing this project. The presence of these people is the essence to success of this project.

My highest appreciation specially goes to the project Supervisor, Mr. Teh Hee Min for his consultation, guidance, concerns, advice and patience in completing this project. I would like to express my gratitude to Miss Koh Moi Ing for her commitment in giving support and advice through out the study.

Ir. Nor Hisham M Ghazali for Department of Irrigation and Drainage Malaysia, and Mr Norhisham from Emas Kiara Sdn Bhd, information and cooperation from both of you are highly appreciated.

Special thank you to Mr. Meor Asniwan, Mr. Idris, Mr. Mohd Zaini Hashim, Mr. Iskandar, and other the lab technicians for giving highest commitment and cooperation in this study especially during laboratory experiments. Humble thanks to the groups of students that has been helping me, giving their hands to help in the laboratory experiments.

Special thanks to my family, for your support and help in term of finance.

Finally, I would like to thank all my friends especially Miss Nabilah Ab. Qahar, Miss Hawa Nuramalina Hussin, Mr. Aidil Ass'ad Anuar and other that have given your support and contribution from the beginning of the study until the end of my study.

Thank you to all that have support me, directly or indirectly. Without all your help, this study may not be finished.

ABSTRACT

Sand container (SC) role in replacing 'hard material' in constructing defense structures has recently being applied and proven to have achieved the desirable performances. A few constructions using this new material have been constructed around the world. This report is written to conclude the finding on "Wave Attenuation Characteristics of Sand Container". The study will focus on the wave attenuation by comparing the wave incident height and the wave attenuation height of these waves which known as transmission coefficient, K_t . A small scale model of sand container has been constructed using cotton fabric. The small scale model is a cylindrical shape with 8 cm of diameter and 30 cm in length. This study is divided into two phases and total of four (4) experiments have been conducted in this study. The study concluded that transmission coefficient, K_t , increases with the increasing of wave period, T , base width, B , water depth, d , f/d , freeboard, f . However, transmission coefficient, K_t , is decreases with the increasing of wave steepness, H/gT^2 , structure height, h , and d/gT^2 . However, in determining the best configuration, all the parameters need to be considered. The best configuration for the study will be the one that will give the lowest value of transmission coefficient, K_t , and is 0.31 at wave period, $T = 0.6$ s, base width, $B = 40$ cm, water depth, $d = 28$ cm, structure height, $h = 26$ cm and freeboard, $f = 2$ cm.

TABLE OF CONTENTS

CERTIFICATE OF APPROVAL	i
CERTIFICATE OF ORIGINALITY	ii
ACKNOWLEDGEMENT	iii
ABSTRACT	iv
TABLE OF CONTENTS	v
LIST OF FIGURES	viii
LIST OF TABLES	xi
CHAPTER 1	1
INTRODUCTION	1
1.1. BACKGROUND OF STUDY	1
1.2. PROBLEM STATEMENT	4
1.3. OBJECTIVES	5
1.4. SCOPE OF STUDY	5
CHAPTER 2	7
LITERATURE REVIEW	7
2.1. INTRODUCTION	7
2.2. SAND CONTAINER	7
2.3. SUBMERGED BREAKWATER	9
2.3.1. SUBMERGED BREAKWATER PRIMARY OBJECTIVES	9
2.4. WAVE DISSIPATION MECHANISM	10
2.4.1. WAVE BREAKING	11
2.5. PREVIOUS STUDY ON WAVE ATTENUATION OF SUBMERGED BREAKWATER STRUCTURE	13
2.6. EXISTING SC UNIT STRUCTURES	16
2.6.1. Artificial breakwater, Narrowneck, Gold Coast, Australia	16
2.6.2. Groyne, North Kirra, Australia	18
2.6.3. Island of Sylt, Germany	19
CHAPTER 3	21
MODEL DESCRIPTION	21
3.1. INTRODUCTION	21
3.2. MODEL DETAILS	21

CHAPTER 4	24
METHODOLOGY / PROJECT WORK	24
4.1. INTRODUCTION	24
4.2. LABORATORY EQUIPMENTS AND INSTRUMENTATIONS	24
4.2.1. Wave Flume	24
4.2.1.1. Wave Generator	26
4.2.1.2. Wave Switch Box	27
4.2.1.3. Wave Absorber	28
4.2.2. Instrument Carriage	29
4.2.3. Hook and Point Gauge	29
4.2.4. Stopwatch	31
4.2.4. Ruler and Marker Pen	31
4.3. EXPERIMENTAL PROCEDURES	32
4.3.1. Frequency Versus Wave Period	32
4.3.2. Wave Period, T Versus Incident Wave Height, H_i	33
4.3.3. Base Width Effect, B and Wave Steepness, H/gT^2 Towards Transmission Coefficient, K_t	33
4.3.4. Water Depth, d , Freeboard, f and Structure Height, h Effect Towards Transmission Coefficient, K_t	34
CHAPTER 5	37
RESULTS AND DISCUSSION	37
5.1. INTRODUCTION	37
5.2. FREQUENCY VERSUS WAVE PERIOD	37
5.3. WAVE PERIOD (T) VERSUS INCIDENT WAVE HEIGHT (H_i)	40
5.4. BASE WIDTH, b AND WAVE STEEPNESS, H/gT^2 EFFECT TOWARDS TRANSMISSION COEFFICIENT, K_t	42
5.4.1. Graph of Transmission Coefficient, K_t versus Wave Period, T	43
5.4.2. Graph of Transmission Coefficient, K_t versus Wave Steepness, H_i/gT^2	44
5.5. WATER DEPTH, d , FREEBOARD, f , AND STRUCTURE HEIGHT, h , EFFECT TOWARDS TRANSMISSION COEFFICIENT, K_t	46
5.5.1. Graph of Transmission Coefficient, K_t versus Wave Period, T	46
5.5.2. Graph of Transmission Coefficient, K_t versus f/d	50
5.5.3. Graph of Transmission Coefficient, K_t versus d/gT^2	55

CHAPTER 6	59
CONCLUSION AND RECOMMENDATION	59
6.1. CONCLUSION	59
6.2. RECOMMENDATION	62
REFERENCES	63

LIST OF FIGURES

Figure 2.1	Typical Submerged Breakwater of a Single Sand Container	10
Figure 2.2	Dimensional variables in determining K_t	11
Figure 2.3	Transmission and Reflection Coefficients versus Structure's Thickness ($\epsilon = 0.8$)	14
Figure 2.4	Transmission and Reflection Coefficients versus Structure's Thickness ($\epsilon = 0.5$)	15
Figure 2.5	Transmission and Reflection Coefficients versus Structure's Thickness ($\epsilon = 0.2$)	15
Figure 2.6	Artificial reef (breakwater), Narrowneck, Gold Coast, Australia	18
Figure 2.7	Groyne at North Kirra, Australia	19
Figure 2.8	The historical house "Kliffende" after the construction	20
Figure 3.1	SCU scale model	22
Figure 3.2	Plan view of SCU	22
Figure 3.3	Side view of SCU	23
Figure 3.4	Front view of SCU	23
Figure 4.1	Wave Flume	25
Figure 4.2	Wave flume components	25
Figure 4.3	Wave generator components	26
Figure 4.4	Wave switch box components	27

Figure 4.5	Wave absorber	28
Figure 4.6	Instrument carriage	29
Figure 4.7	Hook and point gauge components	30
Figure 4.8	Stopwatch, ruler and marker pen	31
Figure 4.9	Unit Location in Wave Flume for Third Experiment	34
Figure 4.10	SC Unit Location in Wave Flume for Fourth Experiment	36
Figure 5.1	Wave Period, T versus Frequency, Hz Graph	38
Figure 5.2	Incident Wave Height, H_i versus Wave Period, T	40
Figure 5.3	Transmission Coefficient, K_t for Corresponding Wave Period, T for Four Base Widths, B	43
Figure 5.4	Transmission Coefficient, K_t for Corresponding Wave Period, T for Four Base Widths, B	45
Figure 5.5	Transmission Coefficient, K_t , for Corresponding Wave Period, T for $h/B = 0.217$	48
Figure 5.6	Transmission Coefficient, K_t , for Corresponding Wave Period, T for $h/B = 0.430$	48
Figure 5.7	Transmission Coefficient, K_t , for Corresponding Wave Period, T for $h/B = 0.650$ (a)	49
Figure 5.8	Transmission Coefficient, K_t , for Corresponding Wave Period, T for $h/B = 0.650$ (b)	49

Figure 5.9	Transmission Coefficient, K_t for Corresponding f/d for $h/B = 0.217$	51
Figure 5.10	Transmission Coefficient, K_t for Corresponding f/d for $h/B = 0.430$	52
Figure 5.11	Transmission Coefficient, K_t for Corresponding f/d for $h/B = 0.650$ (a)	52
Figure 5.12	Transmission Coefficient, K_t for Corresponding f/d for $h/B = 0.650$ (b)	53
Figure 5.13	Wave breaking at wave period, $T = 2.0$ s, freeboard $f = 1.5$ cm	54
Figure 5.14	No obvious wave breaking at wave period, $T = 2.0$ s, freeboard, $f = 7.5$ cm	54
Figure 5.15	Transmission Coefficient, K_t for Corresponding d/gT^2 , for $h/B = 0.217$	56
Figure 5.16	Transmission Coefficient, K_t for Corresponding d/gT^2 , for $h/B = 0.430$	57
Figure 5.17	Transmission Coefficient, K_t for Corresponding d/gT^2 , for $h/B = 0.650$ (a)	57
Figure 5.18	Transmission Coefficient, K_t for Corresponding d/gT^2 , for $h/B = 0.650$ (b)	58

LIST OF TABLES

Table 4.1	Experimental Setup for Third Experiment	34
Table 4.2	Experimental Setup for Fourth Experiment	35
Table 5.1	Wave Period, T for Various Frequencies, Hz	38
Table 5.2	Corresponding Stroke Frequency, Hz versus Wave Period, T	39
Table 5.3	Corresponding Incident Wave Height, H_i versus Wave Period, T ..	40
Table 5.4	Transmission Coefficient, K_t for Corresponding Wave Period, T for Four Dimensionless Base Widths, h/B	43
Table 5.5	Transmission Coefficient, K_t for Corresponding Wave Steepness, H_i/gT^2 for Four Dimensionless Base Widths, h/B	44
Table 5.6	Transmission Coefficient, K_t , for Corresponding Wave Period, T , for $h/B = 0.217$	46
Table 5.7	Transmission Coefficient, K_t , for Corresponding Wave Period, T , for $h/B = 0.430$	47
Table 5.8	Transmission Coefficient, K_t , for Corresponding Wave Period, T , for $h/B = 0.650$ (a)	47
Table 5.9	Transmission Coefficient, K_t , for Corresponding Wave Period, T , for $h/B = 0.650$ (b)	47

Table 5.10	Transmission Coefficient, K_t , for Corresponding f/d , for $h/B = 0.217$	50
Table 5.11	Transmission Coefficient, K_t , for Corresponding f/d , for $h/B = 0.430$	50
Table 5.12	Transmission Coefficient, K_t , for Corresponding f/d , for $h/B = 0.650$ (a)	51
Table 5.13	Transmission Coefficient, K_t , for Corresponding f/d , for $h/B = 0.650$ (b)	51
Table 5.14	Transmission Coefficient, K_t for Corresponding d/gT^2 , for $h/B = 0.217$	55
Table 5.15	Transmission Coefficient, K_t for Corresponding d/gT^2 , for $h/B = 0.430$	55
Table 5.16	Transmission Coefficient, K_t for Corresponding d/gT^2 , for $h/B = 0.650$ (a)	56
Table 5.17	Transmission Coefficient, K_t for Corresponding d/gT^2 , for $h/B = 0.650$ (a)	56

CHAPTER 1

INTRODUCTION

1.1. BACKGROUND OF STUDY

Coastline areas are very important as they have high tourism and economic value especially for countries like Malaysia. Malaysia has about 4,800 km of coastline comprising two distinctly different physical formations, namely the mangrove-fringed mud flats and sandy beaches. The east coast of Peninsular Malaysia consists of straight sandy formations in the north and a series of hook- or spiral-shaped bays to the south. The west coast of Peninsular Malaysia, however, comprises mainly muddy formations, with limited areas of pocket sandy beaches. In Sarawak and Sabah, the coastlines are about equally divided between sandy beaches and mud coast.

The coastal zone is broadly defined as the areas where terrestrial and marine processes interact. These include the coastal plains, deltaic areas, coastal wetlands, estuaries and lagoons. It is difficult to demarcate a fixed geographical limit on the coastal zone due to the complex interaction and inter-dependence of fluvial and coastal processes. The coastal zone of Malaysia has a special socio-economic and environmental significance. It supports large percentage of the population and act as the center of economic activities encompassing urbanisation, agriculture, fisheries, aquaculture, oil and gas exploitation, transportation and communication, recreation, etc.

However, the rapid pace of development activities in the coastal area has resulted in a conflict in the need for immediate consumption and the need to ensure the long-term supply of these resources. This has resulted in a host of problems such as increased erosion areas, siltation, and loss of coastal resources and the destruction of the fragile marine habitat. Defence structures are more likely one of the options to control these problems. There are many defence structures and most of them have

been constructed in Malaysia. Revetment and breakwater are among the popular defence structures constructed in Malaysia.

East coast of Peninsular Malaysia, Sabah and Sarawak are facing the South Chinese Sea, and experienced severe erosion along the coastal zone. The problem of coastal erosion attracted serious attention of the Government in the early 1980s largely as a result of public complaints and pressures. In response, government of Malaysia commissioned the National Coastal Erosion Study in 1984/1985 (Economic Planning Unit, 1985). The study revealed that about 1390 km or 29 % of the coastline were subjected to erosion. Depending on the economic consequence of coastal erosion, these erosion sites were classified under three categories, namely critical, significant and acceptable.

Based on these studies, many defence structures have been constructed. However, building these structures using hard materials has disadvantages. The fact that some of these structures are constructed using a lot of earth rock, causing depletion in the material. Environmentally speaking, these will affect many hilly areas, and also the transportation of the material raising a lot of other issues to public.

Recently, a new technology is implemented, which is by using Sand Container Unit (SCU) instead of rocks and cements. The container can be from various types of fabrics but in the market today, most of them are made of geotextile. The fabric transformed to a sand bag shape and designed to have small circular openings to pump the sand later. These circular holes of about 30 to 45 cm diameter are cut into the top piece of fabric along the center line of the container. Sleeves about 1 meter long are sewn around the holes. The holes serve as access points for filling the tube. Generally, for sands, the filling sleeves should be about 15 to 25 meter apart.

This method of construction is generally much simple compared to using the conventional method. The container unit is filled directly with dredged material from the outflow of a hydraulic dredge. In these applications, the container is created by sewing two sheets of fabric together. The sheets are laid over one another and their edges sewn together. The length of the tube is discretionary. This sand container will

be laid on its position layer by layer to form structure like revetment and breakwater. A few structures around the world have used this material and this material has performed very well. Some of these structures will be discussed in Chapter 2.

1.2. PROBLEM STATEMENT

The historical development of sand containers and its usage for coastal protection was founded in the 1950's. The idea of encapsulating soil as fill material in fabric units is made practical by the high effectiveness and low costs of nonwoven needle-punched filter. With increasing costs of conventional construction materials in hydraulic engineering applications, the use of sand filled containers has increased rapidly. Especially in certain geographic regions with long stretches of sandy beaches and dunes, the possibility of using locally available sand as fill material for individually tailored sand containers provide the main advantage in case of shortage of natural rocks and gravel.

The successful replacing of conventional coastal structural elements made of concrete, ripraps or insufficient available natural materials (e.g. rock) by the use of sand containers in tailored dimensions is followed by new applications wherever construction elements for erosion control, groynes, breakwaters, dune-revetments and scour stabilisation are needed.

In Malaysia, the trend of using the conventional materials has reduced the materials sources. The existing technology which is also known as hard structure; use massive quantity of rocks and/or cements in a single construction. These materials are mainly found inland and thus many quarry areas opened in this inland area to cater the demand for the materials. This resource will someday depleted and not adequate to cater the increased demand. Other issues such as the transportation and high cost also arise. Public safety issues also being raised as far as transporting these materials is concern. This safety issue is being frequently debated in our parliament as it is of public concern.

1.3. OBJECTIVES

The objectives of this study are as follows:

1. To develop sand container models using proper materials.
2. To study the performance of the proposed sand containers via hydraulic model simulation in laboratory.

1.4. SCOPE OF STUDY

The scopes of study for this project are:

1. Literature review

Study and understand the existing sand container developed and marketed worldwide.

2. Development of sand container

Develop a scale model of sand container to be tested in the flume probe. Model used will be the most commonly used in the construction.

3. Laboratory set up

Check the availability of the apparatus and devices used to test the scale modelled structures and checking the accuracy of all devices and performing calibration if necessary.

4. Laboratory test

Test the scale model structures in the wave flume.

5. Result Analysis, conclusion and recommendation

Analyse the results from the laboratory tests done.

6. Thesis write up

Compile the data obtained for the whole project according to the listed format in 'Final Year Project Guidelines' for examiner's evaluation.

CHAPTER 2

LITERATURE REVIEW

2.1. INTRODUCTION

In this project, the performance of the Sand Container (SC) as the material of a submerged breakwater will be analysed. The performances of the sand container unit (SCU) will be on the wave attenuation due to this SC-type submerged breakwater. This chapter will focus on the analytical, critical and objective review of sand container and submerged breakwater. This chapter also provides the background information on the study and highlights some of existing structures that use the SCU as the main material.

2.2. SAND CONTAINER

Sand container has recently become a new engineering technology with numerous applications. One of these applications is the use of container filled with a slurry-mix, including sand, concrete, or mortar for revetment, groyne or breakwater.. These containers have proven to be an economical alternative for the construction of breakwaters, groins, and temporary levees. They have also been used for slope protection along with many other engineering projects.

This container can be made of various fabrics which should meet the construction requirement. If the sand container were about to hold water or runoff from river, it must use a non-permeable fabric. However, in this study, the main focus fabrics are those that used for submerged breakwater construction, which is using permeable fabric like geotextile. These containers are able to hold back materials while water flows through. Geosynthetic containers are large containers consisting of a woven geotextile material filled with a slurry-mix. The mix usually consists of dredged material from the nearby area but can also be a mortar or concrete mix. These containers are generally about 1 m to 2 m in diameter, though

they can be sized for any application. The container can be used solely, or stacked to add greater height and usability. They can be constructed of any length depending on the use. The most used fabric in constructing the permeable sand containers is geotextile.

Geotextile has very high durability, water-permeable and filter-stable (Kohlhase, 1997). Massive studies were made and lead to acknowledgement as being state of the art for the use of filtration and revetment purposes in hydraulic engineering. Their lifetime for long term stability corresponds to the usual planned lifetime of the coastal work. The geotextile performance of filtration, separation, drainage and reinforcement has led to the idea of designing geotextile sand containers, where needle-punched function as the containment for local available soil materials. These geotextile sand containers provide soft and flexible coastal solutions and have less permanent impact on the environment, which is the advantage over massive and hard construction elements made of concrete, steel or rocks. The contained material is not subject to erosion during and after placing and sand containers can be filled and placed with a variety of simple or complicated equipment.

Geotextiles consist of needle-punched short fibres which is UV-stabilised polyester-fibres, with a pore distribution in three dimensional directions. The pore structures of geotextiles (approximately 90% pore volume) behave better than natural granular filters (approx. 50% pore volume). Even if the major part of the pore structure is filled by soil particles during the lifetime of a coastal structure, the permeability is not reduced to such an extent that pressure gradients within the filter layer are noticeable increased. Long-term stable filter have a comparable ability to deform.

For coastal protection measures, geotextile is proven being resistant against ultraviolet radiation and saltwater (Heerten, 1980). High elongation behaviour provides the superior properties during the construction load case, which is determined as being the biggest risk for damaging the geotextiles. With a reputation of providing high robustness and abrasion resistance, a geotextile container – if possible filled with locally available soil material can be used in nearly every hydraulic construction project where conventionally gravel, stones or rocks are used.

Additionally, using geotextile sand containers possibly helps to save gravel resources. Transportation of these materials, which often have to be delivered to the site from distant areas, is avoided since classified fill material is not required

2.3. SUBMERGED BREAKWATER

In this study, the sand container is used to construct a submerged breakwater. Breakwater is a structure protecting a shore area, harbour, anchorage or basin from waves (Shore Protection Manual, Third Edition, 1977). This structure mainly serves as an aid to navigation, a shore-protection structure or a trap for littoral drift. The purpose is to reduce the hydraulic loading to a required level that maintains the dynamic equilibrium of the shoreline. In attaining this goal, it is designed to allow the transmission of a certain amount of wave energy over the structure by overtopping and also some transmission through wave breaking and energy dissipation.

2.3.1. Submerged Breakwater Primary Objectives

The submerged breakwater is not designed to fully block the wave energy and longshore current from reaching the shoreline. Instead, it will minimize these energy and current to a certain level and maintain the shoreline beach from erosion. Submerged breakwater primary objectives are as follows:

1. Improve the recreational value of the windward beach by reducing the wave energy sufficiently to allow the creation of a stable new beach using natural sand, replacing the existing coarse dredge spoil beach.
2. Maintain sufficient environmental flow and water exchange behind the breakwater to ensure the survival of existing marine life.
3. Provide wave attenuation to reduce the average turbidity of the water to enhance water quality.
4. Minimize visual impact by remaining below the waterline.
5. Provide guided snorkelling and diving trails with maximum diversity and abundance of marine life.

6. Minimize the loss of existing marine life within the footprint of the breakwater.
7. Mimic as closely as possible a natural fringing coral reef system.

2.4. WAVE DISSIPATION MECHANISM

The submerged breakwater deals directly with wave breaking, wave transmission and energy dissipation to allow the wave attenuation. These wave actions will determine the effectiveness of the SC-type submerged breakwater.

The main parameters used to describe the general geometry of a submerged breakwater are shown in Figure 2.1. These include the height of the structure = h , water depth at the toe of the structure = d , and the freeboard of the structure = F , where the freeboard is the difference between the height of a breakwater structure and the water depth at the seaward toe of the structure.

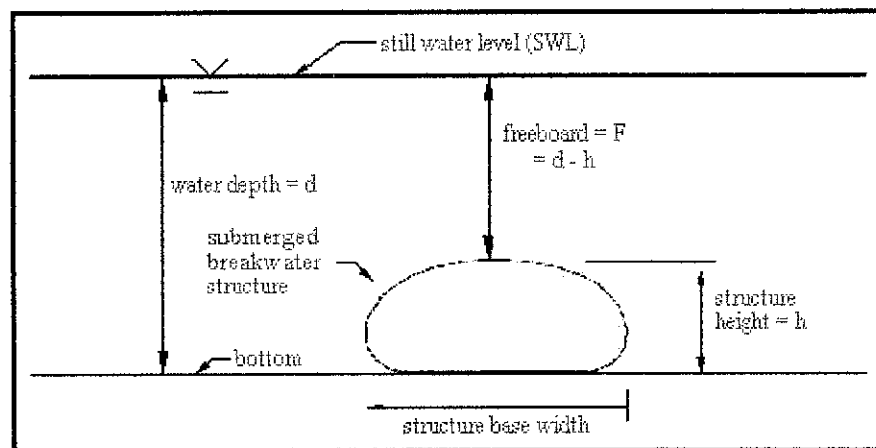


Figure 2.1: Typical Submerged Breakwater of a Single Sand Container

2.4.1. Wave Breaking and Wave Transmission

Wave breaking is one of the most commonly observed features of water waves. Breaking is always a nonlinear phenomenon and is therefore extremely difficult to describe analytically. As a wave propagates into intermediate and shallow water, an initial profile asymmetry develops around the horizontal axis as the wave crest steepens and the wave trough flattens. The reduction of the wave velocity due to wave propagation and reduction of wave length (due to different water depth) will contribute to wave breaking.

The efficiency of submerged structures and the resulting shoreline response mainly depends on transmission characteristics and the layout of the structure. In other word, wave transmission is basically the wave life travel after it reaches the submerged breakwater; which also will be the part of the energy dissipation system. A number of engineering procedures to estimate combined wave transmission through a breakwater and wave overtopping are available, but still not very reliable. The transmission coefficient, K_t , defined as the ratio of the height directly shoreward of the breakwater to the height directly seaward of the breakwater, has the range $0 < K < 1$, for which a value of 0 implies no transmission (high, impermeable), and a value of 1 implies complete transmission (no breakwater).

Factors that control wave transmission include crest height and width, structure slope, material (permeability and roughness), tidal and design level, wave height and period. As wave transmission increases, diffraction effects decrease, thus decreasing the size of a salient through direct attack by the transmitted waves and weakening the diffraction-current moving sediment into the shadow zone. It is obvious that the design rules for submerged structures should include a transmission coefficient as an essential governing parameter.

The primary purpose of a breakwater is to reduce the wave energy in its lee. The term “wave transmission” is used in reference to the wave energy that does travel past a breakwater, either by passing through and/or by overtopping the structure. The wave energy that is attenuated in the lee of the breakwater is either dissipated by the structure (such as by friction or wave breaking) or reflected back as reflected wave energy.

The effectiveness of a breakwater in attenuating wave energy can be measured by the amount of wave energy that is transmitted past the structure. The greater the wave transmission coefficient is, the less the wave attenuation. Wave transmission is quantified by the use of the wave transmission coefficient,

$$K_t = \frac{H_t}{H_i} \quad \text{Equation 1}$$

where K_t is the wave transmission coefficient, H_t is the height of the transmitted wave on the landward side of the structure, and H_i is the height of the incident wave on the seaward side of the structure

The equation above is derived from dimensional analysis (Sharp, 1981), which dimensional variables that influences the wave transmission K_t can be expressed as follows, referring to Figure 2.2:

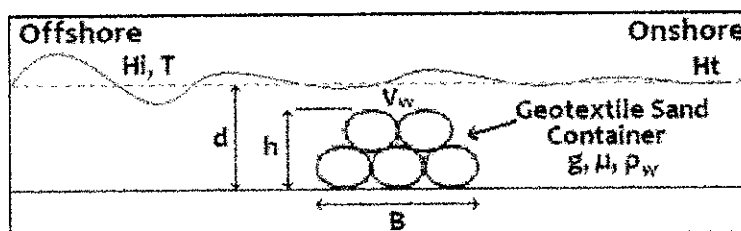


Figure 2.2: Dimensional variables in determining K_t

$$K_t = \frac{H_t}{H_i} = f[h, T, \rho_w, H_i, H_t, d, B, V_w, \mu, g] \quad \text{Equation 2}$$

ρ_w , μ , and V_w is the mass density, dynamic viscosity, and typical velocity of water in the vicinity of reefs, while g is the gravitational acceleration. Solving equation above by the matrix method (Sharp, 1981) produces the following π terms:

$$\frac{H_i}{h}, \frac{H_t}{h}, \frac{d}{h}, \frac{B}{h}, \frac{V_w T}{h}, \frac{\mu T}{h^2 \rho_w}, \frac{g T^2}{h} = \pi_1, \pi_2, \pi_3, \pi_4, \pi_5, \pi_6, \pi_7$$

Equation 3

By compounding the π terms

$$\frac{H_i}{gT'} \frac{H_t}{H_i} \frac{h}{d'} \frac{h}{B'} \frac{V_w T'}{h} \frac{V_w h}{\mu/\rho_w} \frac{V_w^2}{gh} = \frac{\pi_1}{\pi_7} \frac{\pi_2}{\pi_1} \pi_3^{-1} \pi_4^{-1} \pi_5 \frac{\pi_5}{\pi_6} \frac{\pi_5^2}{\pi_7}$$

Equation 4

The first four terms explains the properties of the incoming and transmitted waves, structure placement and geometry, namely: wave steepness, wave transmission, depth submergence, and reef proportion. The last three parameters are the Keulegan-Carpenter (KC) number, Reynolds number and Froude number which are important in similitude analysis of hydraulic and turbulent modeling (Hughes, 1993). When the last three terms are considered constant, thus:

$$K_t = \frac{H_t}{H_i} = f \left[\frac{H_i}{gT'^2}, \frac{h}{d'}, \frac{h}{B'} \right] \quad \text{Equation 5}$$

2.5. PREVIOUS STUDY ON WAVE ATTENUATION OF SUBMERGED BREAKWATER STURCTURE

For submerged breakwater system, Newman (1965) analyzed the propagation of water waves past long impermeable obstacles in an infinite water depth. They found that for $kh_s > 0.1$ (k is the wave number, and h_s is the depth of submergence) the transmission coefficient was always larger than 0.8. Mei and Black (1969) studied infinitesimal surface waves normally incident upon a rectangular impermeable obstacle in a channel of finite depth. They found that for a thin obstacle with a depth of submergence of 1/5 times water depth the transmission coefficient can be larger than 0.9. Dick and Brebner (1968) conducted experimental studies on solid and permeable submerged breakwaters.

It was found that for a thin submerged impermeable breakwater with a depth of submergence of only 0.075 times water depth, the transmission coefficient could reach a value of up to 0.9. However, it was added that the transmission coefficient could be reduced by increasing the structure's crest width. Dick and Brebner

indicated that at the same depth of submergence the transmission coefficient could be lowered down to 0.3, if the crest has a width of half of a wavelength. In addition, it was claimed that for depth of submergence $>5\%$ of water depth, a submerged permeable breakwater transmits less wave energy than the solid one over a certain frequency range. Even so, they found that for a submerged permeable breakwater with a porosity of 0.4, and for which the depth of submergence was 0.2 times water depth and crest width was $1/2$ wavelength, the transmission coefficient could be still larger than 0.5. Rojanakamthorn et al. (1989) performed both theoretical and experimental investigations on wave transformation over a submerged permeable breakwater. Their breakwater had a porosity of 0.39, and studies were performed at two depths of submergence (0.2 and 0.3 times water depth). Results showed that the transmission coefficient ranged from 0.1 to 0.7 depending on wave conditions and physical features of the structure.

Sheng-Wen Twu, Cheng-Chi Liu, and Wen-Hung Hsu has conducted a series of tests to study the Wave Damping Characteristics of Deeply Submerged Breakwaters. In their theoretical analysis, the complex Eigen function approach was employed. They define submerged breakwater to be a rectangular form and vertically stratified with multislice porous material. They performed theoretical computations for both single-slice (nonstratified) and multislice submerged breakwaters. Half of the water depth is selected as the submergence of the breakwater.

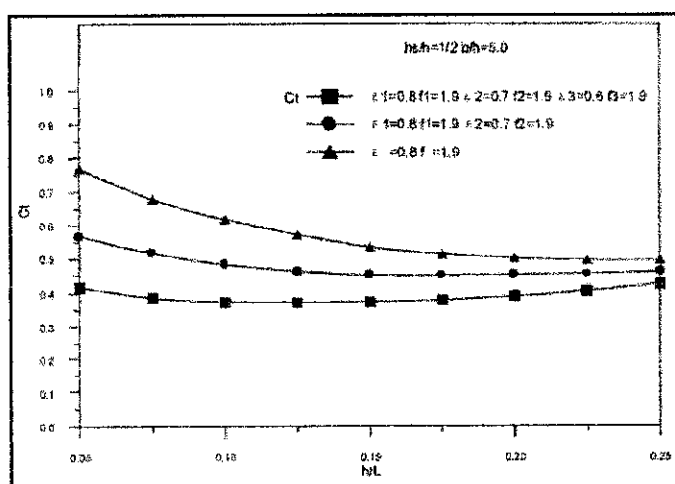


Figure 2.3: Transmission and Reflection Coefficients versus Structure's Thickness ($\epsilon = 0.8$)

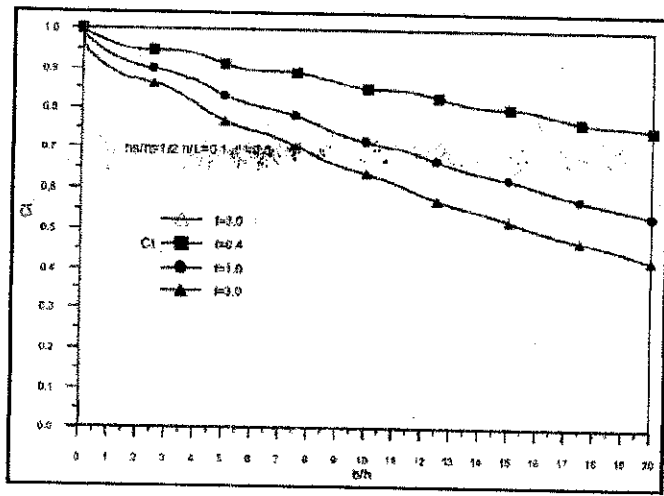


Figure 2.4: Transmission and Reflection Coefficients versus Structure's Thickness ($e = 0.5$)

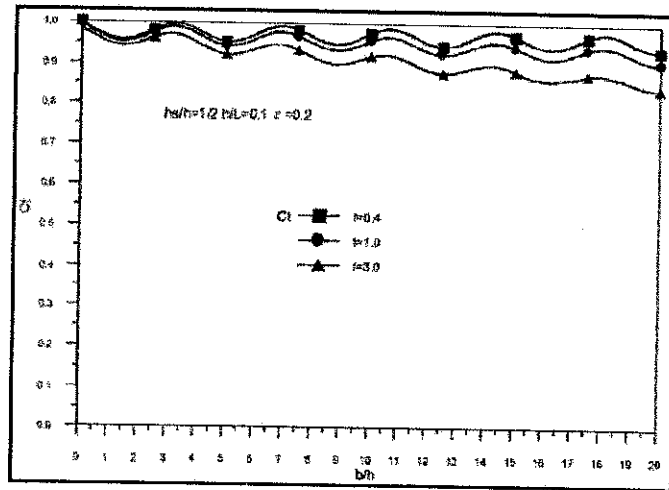


Figure 2.5: Transmission and Reflection Coefficients versus Structure's Thickness ($e = 0.2$)

In this study, they concluded that the computational results show that, for a single-slice breakwater, the transmission coefficient could be effectively reduced, while the porosity of structure material is as high as 0.8 and the thickness-depth ratio $b/h = 20$ (b is the structure thickness, and h is the water depth). A large transmission coefficient can be predicted for a deeply submerged breakwater without sufficient thickness-depth ratio. However, this problem could be improved by adopting a

multislice structure concept in which the breakwater structures with more slices are more effective in reducing the transmission coefficient.

2.6. EXISTING SC UNIT STRUCTURES

Even though the SC technology is about just 50 years old, there are many structures in the world that used this type of materials that recognised and being benchmarks as successful structures. Some of these structures are:

2.6.1. Artificial breakwater, Narrowneck, Gold Coast, Australia

Narrowneck is located Surfers Paradise and Main Beach, Gold Coast, Queensland. This location is facing open surf beach with an offshore max wave height of more than 12m. The reef (see Figure 2.6) is an integral part of the Northern Gold Coast Beach Protection Strategy whose aim was to widen and protect the northern beaches as well as enhancing the surfing amenity. The reef will provide a low profile, near shore control point to retain approximately 80,000 m³ p.a. of the 500,000 m³ p.a. of sand transported to the north along this shoreline. The public supported a user friendly structure.

A condition of approval was for modification and even total removal if required. The mega sand containers facilitated these requirements. The mega sand containers were constructed from heavy duty polyester Terrafix® non woven geotextile. Nearly 400 mega sand containers varying from 3.0 meters to 4.6 meters in diameter, were placed using a split hulled, trailing suction hopper dredge fitted with computer interfaced DGPS. The containers were accurately filled utilising a calibrated density meter, ensuring repeatability.

The ability to fill to a pre-determined shape and accurately place very large containers at a very low unit cost was conclusively proven. Damage occurred to some container during lying and very effective underwater patching techniques were developed. Various coatings were trialed for the crest bags with mixed success but towards the end of the construction a durable composite material was developed and tested with great success. Although some top up is still required, monitoring has

shown a clear salient at times and enhanced surfing conditions. The results from the techniques developed for this project have given confidence for other reef projects to proceed.



Figure 2.6: Artificial reef (breakwater), Narrowneck, Gold Coast, Australia

2.6.2. Groyne, North Kirra, Australia

The location is facing the open surf beach with an offshore max wave height of more than 12m. A temporary structure was needed to retain nourishment to restore the eroded beach, whilst long term nourishment solutions were resolved to restore the long eroded southern Gold Coast beaches. The eroded conditions of these beaches had long been associated with the economic down turn of the immediate area due to poor tourism figures. As the site is a popular surfing area with a local surf life saving club, the structure had to be safe for swimmers and surfers. It also needed to be removable if necessary after a permanent solution was implemented.

The sand filled 120m long x 5m high sand filled groyne (see Figure 2.7) was constructed of 100m long tubes encapsulated in envelopes. To minimise risk during construction, and to allow for erosion of the seabed after construction, the groyne was constructed in a de-watered excavation following initial beach nourishment. This construction technique required all weather, around the clock program, utilising a six inch suction dredge pumping a series of one meter diameter non-woven container that in turn were completely encapsulated in layered diaphragms. The project was ambitious in regards to the size of the structure and location in an active surf zone.

Conventional armour units were not an acceptable option due to the cost and difficulty associated with the ultimate removal of rock or concrete. This groyne was a success in terms of achieving its primary objective of a safe temporary structure for beach stabilisation despite damage to the seaward end due to vandalism. The groyne length was reduced by about 20m before it was completely covered by a regional nourishment scheme commenced in 1990. The experience with vandalism leads to trials of coatings such as bitumen and early patching techniques. As the risk of damage is greater with tubes there has been a trend away from tubes to smaller containers to isolate any damage. Tubes still have an application and the techniques developed at North Kirra have been utilised on other tube projects.

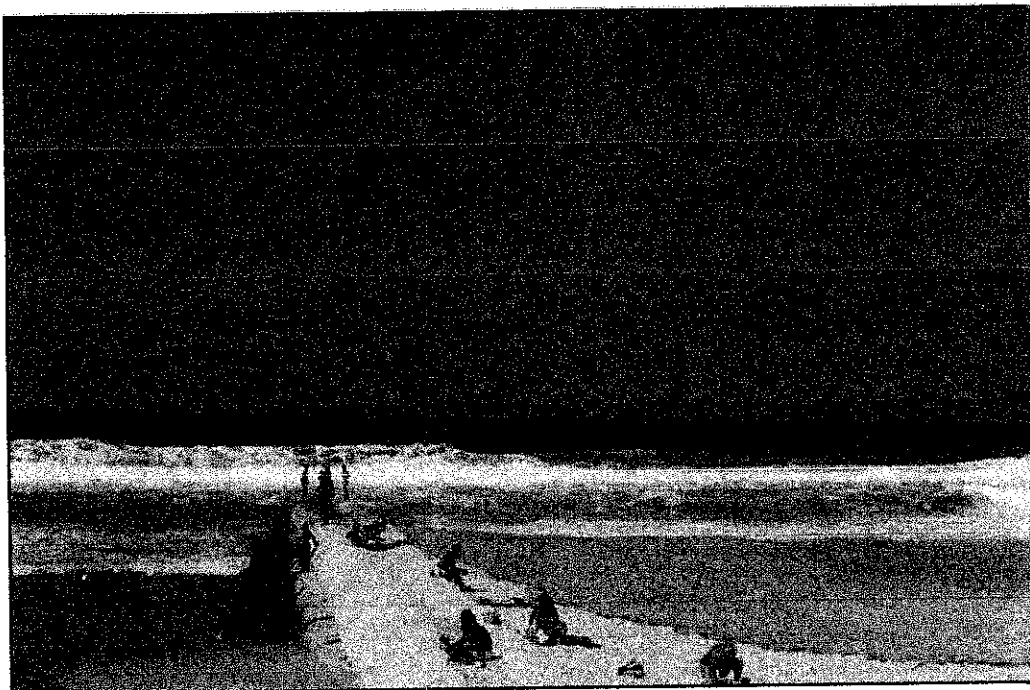


Figure 2.7: Groyne at North Kirra, Australia

2.6.3. Island of Sylt, Germany

At the beginning of 1990, a series of storm tides had caused severe erosion to the west coast of Sylt. After this event, the historical house “Kliffende” was only 5.40 m away from the edge of the cliff. Originally, it was about 80m from the edge of the cliff. There was a big danger that the west gable of the house would fall into the sea during one of the next storm tides and that the house would thus suffer irreparable damage.

Consulting engineers developed a new system consisting of “sand cushions” (see Figure 2.8). In this construction, geotextile fabric is used. The installed containers fulfil the two requirements. On the one hand the geotextiles function as a filter-effective protection against sediment wash-out and on the other hand the terraced layered geotextiles work as reinforcement for stabilisation of the dune embankment. In combination with beach nourishment this construction was designed as “2nd defense line” and sand should be covering the structure again after severe eroding winterstorm periods.

A very specially designed needle-punched composite consisting of a polypropylene slit film woven and a polyester non-woven was selected. The achieved total height of the construction is 8m with inclinations of (V:H=) 1:2 in the lower and (V:H=) 1:4 in the upper cross section area. The seaward faces of the sand cushions were accurately formed with the aid of concrete shuttering elements. Transverse bulkheads were provided by installing fabric/non-woven sheets in order to counteract possible scouring of sand from the sides in case of partial damage to the construction.

The structure proved worthwhile several times during winter storms in 1993 and 1994. The geotextile construction was exposed during these storm tides, but not damaged. The Terrafix Soft Rock[®] construction even survived the second largest storm surge at the west coast of Schleswig-Holstein on December 3 and 4, 1999, showing superior effectiveness compared to all other structures being used on the island. Thus the geotextile structure survived storm surges with a still water level at 2.5m above normal and severe wave action which could reach more than 5.0m.



Figure 2.8: The historical house "Kliffende" after the construction

CHAPTER 3

MODEL DESCRIPTION

3.1. INTRODUCTION

A small scale model of the sand container (SC) is constructed to be tested in the Coastal and Hydraulics Laboratory of UTP. In this chapter, the details of SC model used in the experiment will be explained. Through extensive literature review in Chapter 2, the most suitable shape for the sand container is a cylindrical shape (see Figure 3.1, 3.2, 3.3 and 3.4).

3.2. MODEL DETAILS

For this research purposes, the primary affecting parameters for wave energy dissipation in the experiment are the water depth, wave incident and also the arrangement of the SCU. Below are the specifications of the scale model SCU that will be throughout the laboratory experiment

1. SCU dimension : Square of diameter 8 cm and 30 cm long
2. Material : Cotton fabric
3. Sand size : 50 micron meter -- 2 millimeter
4. Sand volume : 1150 – 1250 cm³ (80-85% full)
5. Weight : 1.8 - 2.0 kg

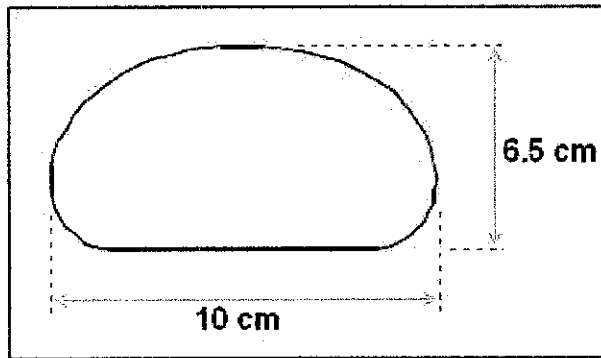


Figure 3.1: SCU scale model

Figure 3.2, 3.3 and 3.4 shows a small scale SCU which is made of cotton that has been constructed. For a small sand container, the commonly design diameter is about 1 meter. The scale down model is 1:12.5 (as 8 cm to 100 cm of diameter).

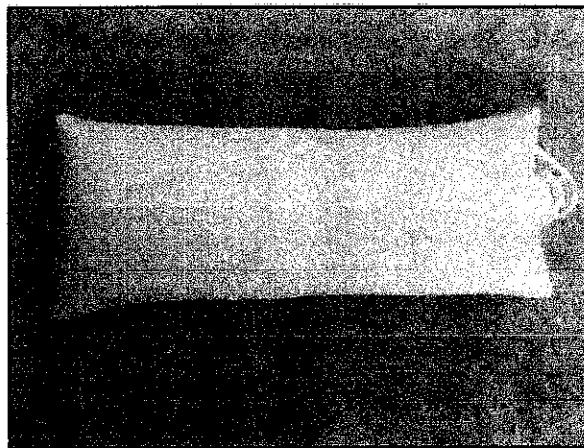


Figure 3.2: Plan view of SCU

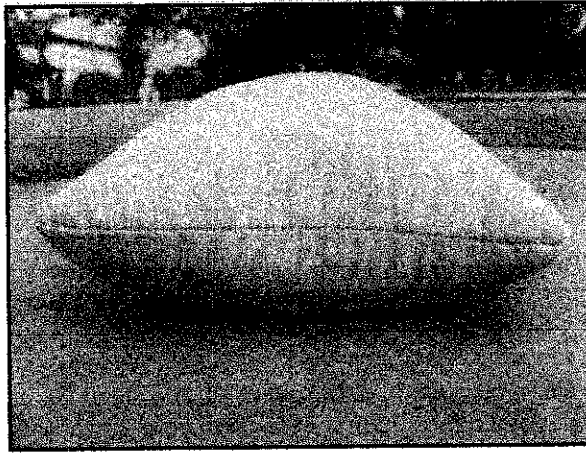


Figure 3.3: Side view of SCU

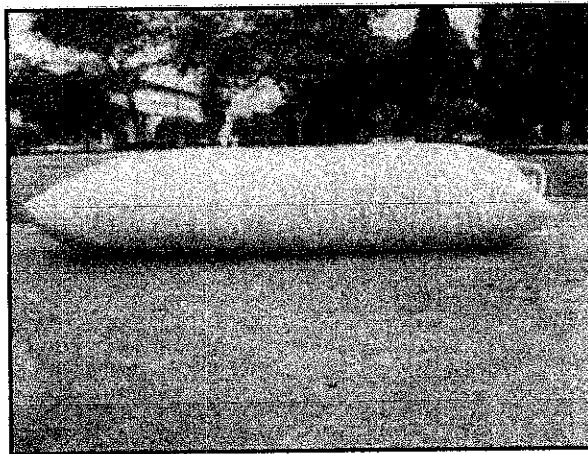


Figure 3.4: Front view of SCU

CHAPTER 4

METHODOLOGY

4.1. INTRODUCTION

All experimental works were carried out in the Coastal and Hydraulics Laboratory of UTP. This chapter will explain the equipments and instrumentations to be used through out the laboratory experiments. This chapter also will explain the experiments procedures that will be carried out. For first phase of study, two preliminary experiments will be carried out. The first experiment will be conducted to determine the wave period (T) with respect to different frequencies. The second experiment is to measure the incident wave height (H_i) for different wave period (T) in different water depths (d). Continuing the second phase of study is third experiment, to determine the base (b) of SC unit effect towards the K_t value. Fourth experiment is to determine the water depth (d) effect towards the K_t value.

4.2. LABORATORY EQUIPMENTS AND INSTRUMENTATIONS

4.2.1. Wave Flume

The wave flume used in the laboratory is Modular Flow Channel HM 162. The wave flume has the dimension of 10 meter long, 0.30 meter wide and 0.45 meter high. It has rigid steel bed and two walls lined with glass panel for the entire length of the flume (see Figure 4.1). This will give clear observation and non-obstructive view of the processes inside the flume.

This wave flume has three main parts (see Figure 4.2) which are:

1. Wave generator
2. Wave switch box
3. Wave absorber

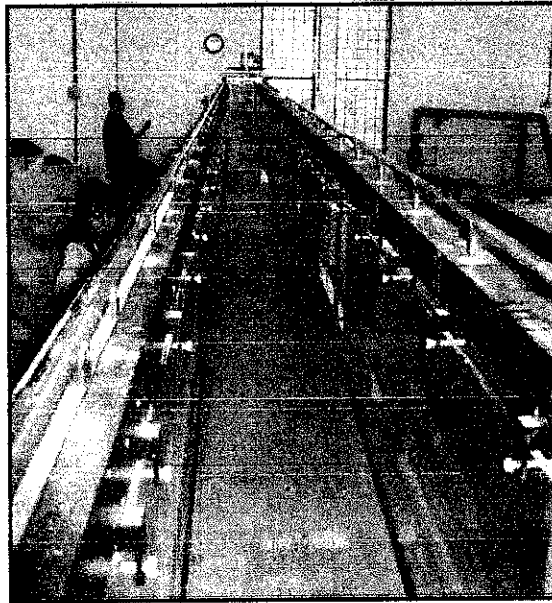


Figure 4.1: Wave Flume

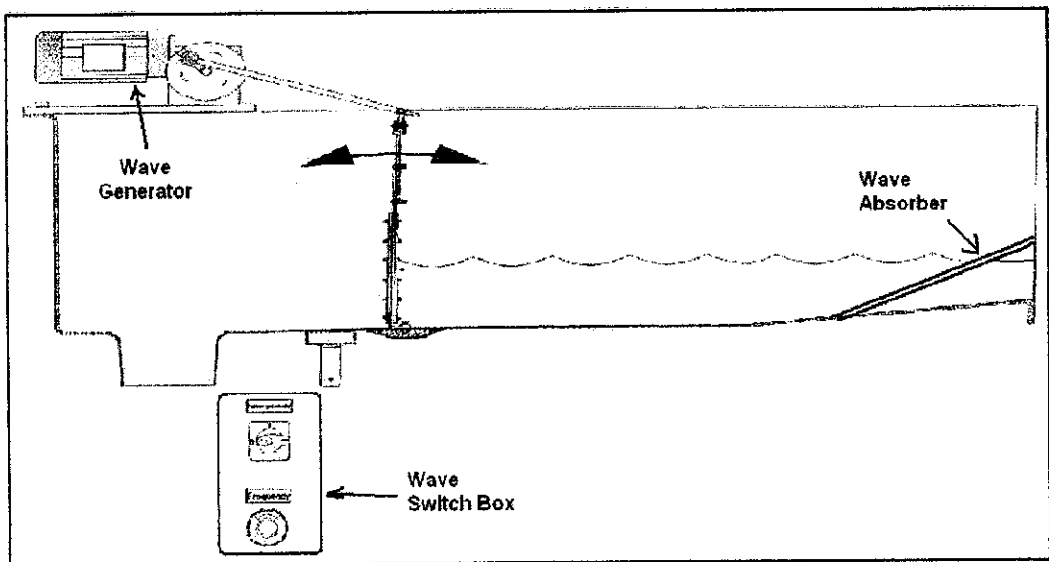


Figure 4.2: Wave flume components

4.2.1.1 Wave Generator

Wave generator used in the laboratory is Wave Generator HM 162.41. Wave generator used to generate regular monochromatic waves with a range of period. The wave generator is bolted onto the surrounding edge of the outlet element of the wave flume. The push rod is connected to the holder of the movable overflow weir. The wave generator is driven by a worm gear motor. The rotational speed can be steplessly varied by a frequency converter and potentiometer. The rotary movement of the motor is converted into a harmonic stroke motion of the movable overflow weir via a crank disk with push rod. The wave generator components are as indicated in Figure 4.3.

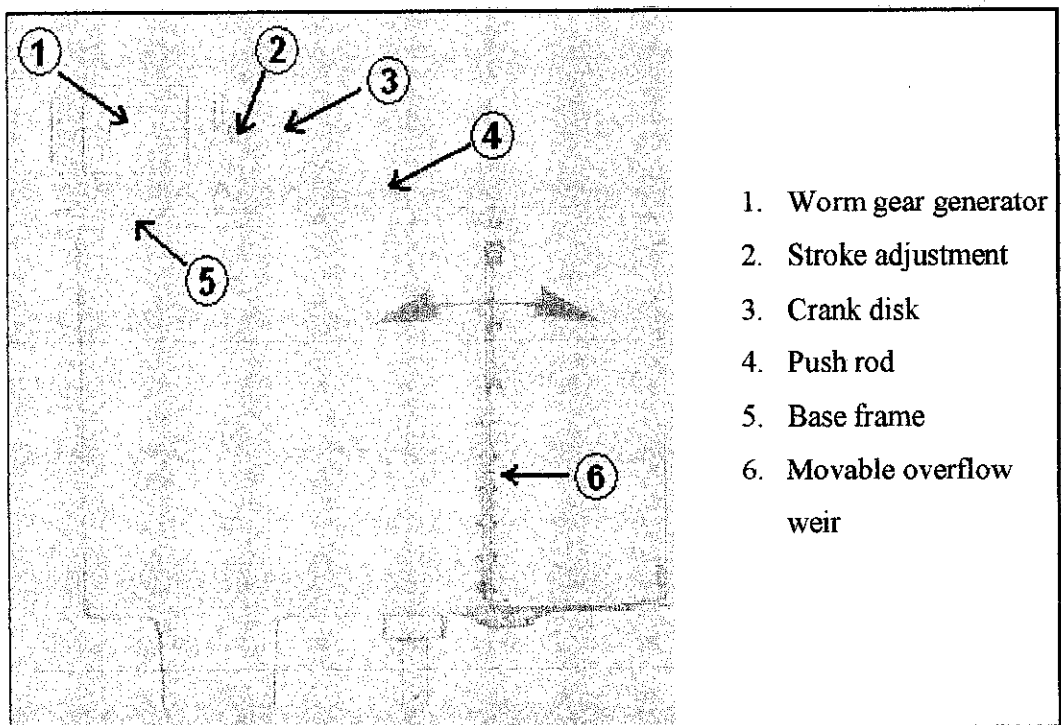


Figure 4.3: Wave generator components

4.2.1.2. Wave Switch Box

The wave switch box function is to operate the wave paddle according to the stroke frequency set in the system. Before any operation, it is important to make sure that the cam switch is set to 0/off position. The rational speed gives the stroke frequency of the wave generator and can be adjusted via a 10-gear helical potentiometer. The potentiometer has a scale disk for guaranteeing assignment of the rotational speed. Thus, some calibration needs to be made. The wave switch box components are as shown in Figure 4.4.

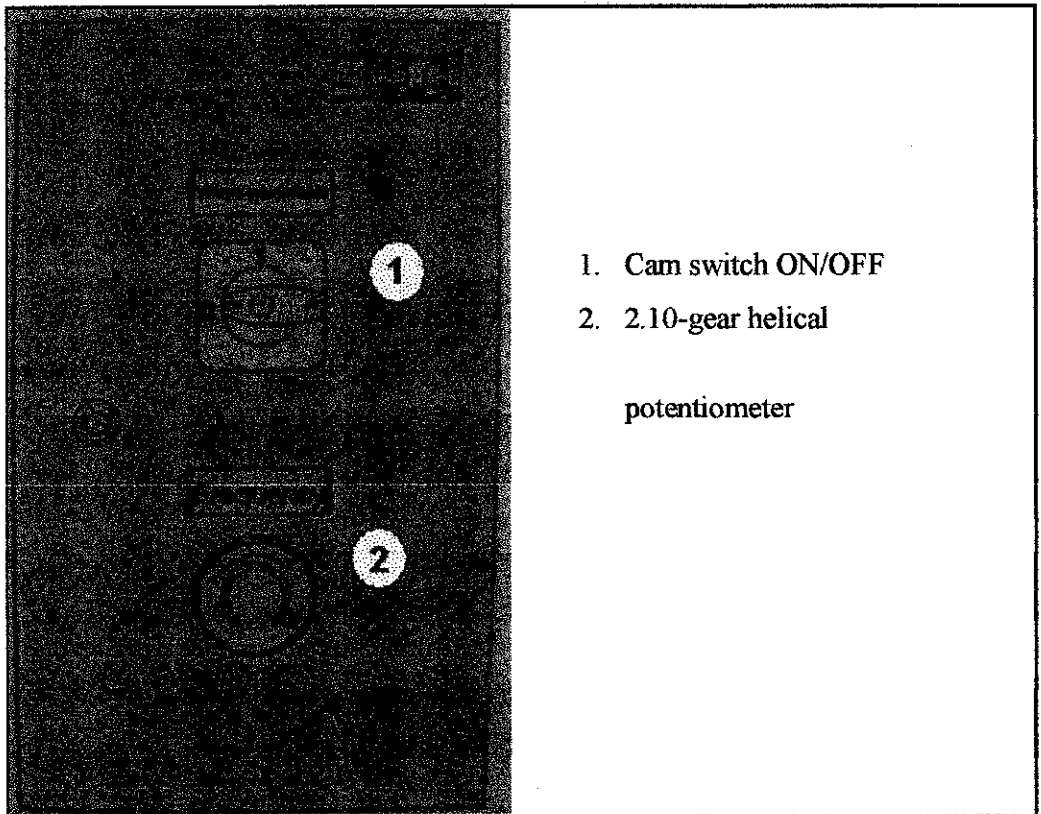


Figure 4.4: Wave switch box components

4.2.1.3. Wave Absorber

Wave absorber as shown in Figure 4.5 is located at the end of the flume probe. Wave absorber is installed to absorb the energy of the incoming waves thereby, reducing the reflected waves from interfering with the incoming waves in the wave flume. The effect of reflection waves in the flume is undesirable and can cause the measured data prone to error.

Wave absorber is made of plastic wire meshes with adjustable slope angle from 0° to 90° . The dimension of the wave absorber is 120 cm length and 30 cm width.

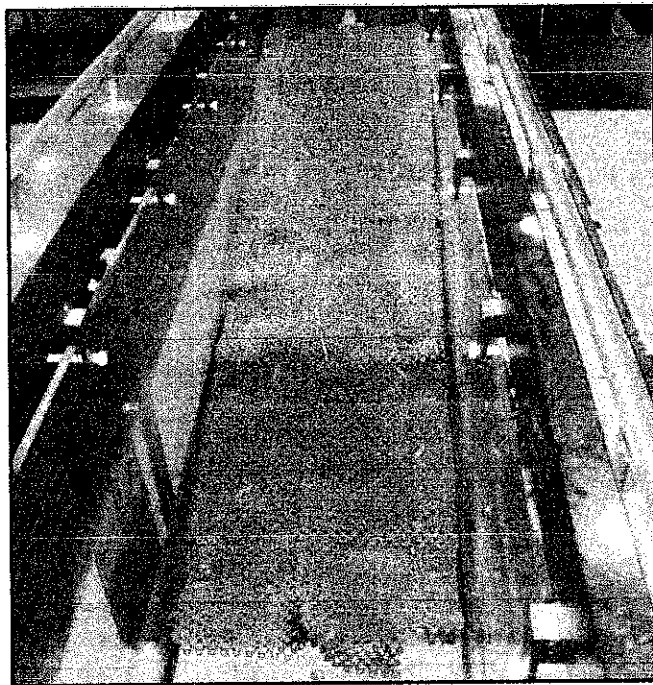


Figure 4.5: Wave absorber

4.2.2. Instrument Carriage

The instrument carriage as shown in Figure 4.6 was designed as a holder for additional accessory unit. The dimension of the instrument carriage is 43 cm long, 35 cm width and 14 cm height and having weight of approximately 4 kg. It can moves to almost any point within the working area of the flume probe. A longitudinal and transverse scale with mm markings permits precise positioning of the instrument holder. Two most common accessory units are the Pitot Static Tube and Level Gauge.

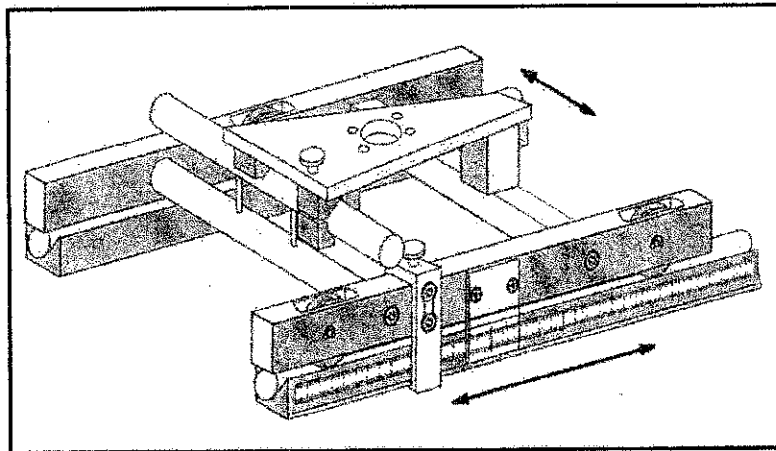


Figure 4.6: Instrument carriage

4.2.3. Hook and Point Gauge

The hook and point gauge is used to measure the water level at any point in the operating range of the wave flume. The relevant position is read of at three different points on the gauge. The three read off point are for the travel width, travel length and height setting. All the three read off points and other components of the hook and point gauge are as shown in Figure 4.7.

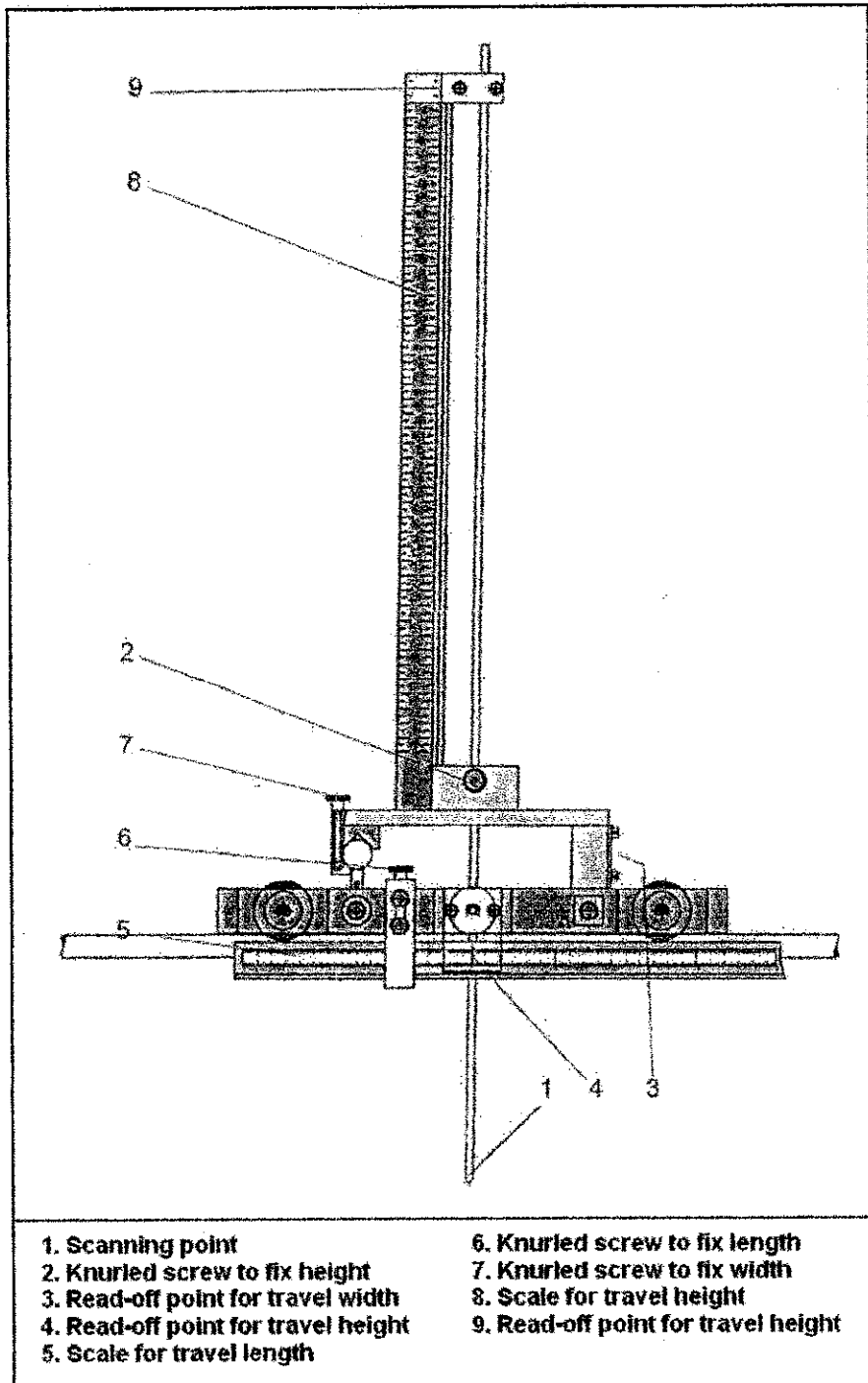


Figure 4.7: Hook and point gauge components

4.2.4. Stopwatch

Stopwatch (see Figure 4.8) is used to measure the wave period of frequency during the experiment

4.2.5. Ruler and Marker Pen

Ruler and marker pen (see Figure 4.8) are used to take the reading of wave height during the experiment. Marker pen is used to mark the crest and trough of the wave and the ruler to measure the height of the two points.

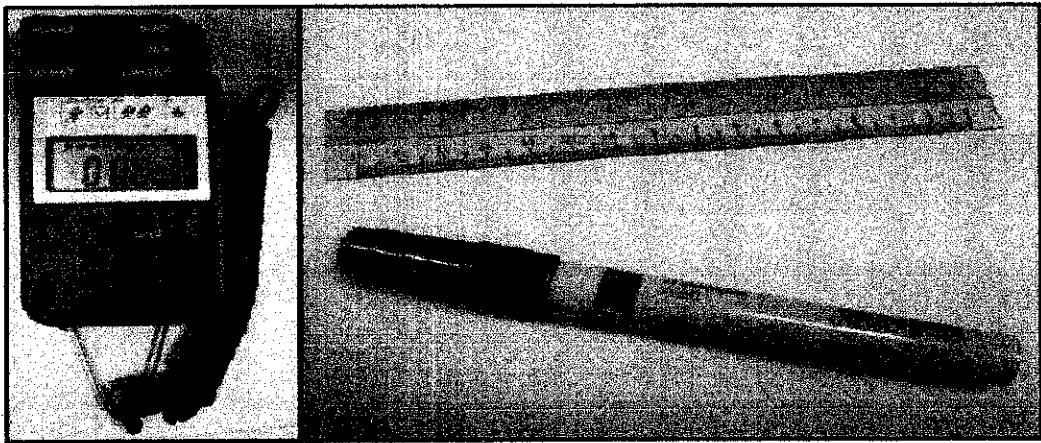


Figure 4.8: Stopwatch, ruler and marker pen

4.3. EXPERIMENTAL PROCEDURES

Throughout the experiment the stroke adjustment was set to be at 180 mm. This ensures the generation of constant wave height at a particular water depth is achieved. During the first phase of this study, two experiments will be conducted. The first experiment is carrying out to determine the relationship between wave period (T) and the stroke frequency of the wave generating system. The second experiment is to determine the incident wave height (H_i) of the flume at different water depths.

Continuing the second phase of study is the third experiment, to determine the base of SC unit effect towards the K_t value. Fourth experiment is to determine the water depth effect towards the K_t value.

The last three parameters are the Keulegan-Carpenter (KC) number, Reynolds number and Froude number which are important in similitude analysis of hydraulic and turbulent modeling (Hughes, 1993). When the last three terms is considered constant, thus:

$$K_t = \frac{H_t}{H_i} = f \left[\frac{H_i}{gT^2}, \frac{h}{d}, \frac{h}{B} \right]$$

4.3.1. Frequency Versus Wave Period

As previously discussed in section 4.1, several operation defects of the wave generating system have been detected prior to the actual experiment done in the wave flume.

In this experiment, different frequencies are set at the potentiometer and times for the crank disk to make 10 cycles were determined. One cycle of crank disk will form one wave length and thus also gives the wave period (T) for the given frequency. The potentiometer will set how many rotation the crank will rotate in a minute. Thus, the first test which is meant to calibrate the frequency set at the potentiometer with the time needed for the crank fully made a rotation.

Stopwatch is used to record the time taken for the crank disk to revolve 10 cycles. The idea of this experiment is to get the wave period of the waves with the given set of frequency value. Frequencies are varied from 20 Hz to 100 Hz with an interval increment of 5 Hz. After setting the frequency at the potentiometer, the device is turned on and time taken for the crank disk rotating 10 cycles is recorded. The experiment is repeated three times for each wave frequency. The wave period (T) is determined by averaging time recorded for each sets of frequency and divided by 10 to obtain the averaged wave period.

4.3.2. Wave Period, T versus Incident Height Wave, H_i

This experiment is meant to determine the incident wave height (H_i) for five different wave periods (T) in thirteen (13) different water depths (d). Water depths have been selected in this experiment is as shown in Table 4.1. The experiment was done prior to the installation of model in the flume probe.

After setting the frequency (for given time period), the device is turned on and series of waves is developed. Incident wave height (H_i) is wave height from the trough to crest of the wave. Measurements were taken at three different locations at the test section of the flume. The incident wave height for each frequency is determined by averaging the three readings.

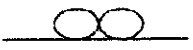
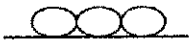
4.3.3. Base Width Effect, B and Wave Steepness, H_i/gT^2 Towards Transmission Coefficient, K_t

This experiment is carried out to determine the transmission coefficient (K_t) for given base width by using five (5) wave periods for each scenario. This is done by determine the transmission wave height (H_t) for each scenario and divide by the respective incident wave height (H_i) that has been determined in the second experiment.

Four different base width of structure are determined: 10, 20, 30 and 40 cm with constant water depth of 10 cm. Height of the structure is 6.5 cm. The experiment is done using wave period of 0.6 second and six readings are recorded. The height of transmission wave (H_t) is taken at 50 cm distance behind the structure. The experiment is repeated using wave period of 0.6, 1.0, 1.3, 1.6 and 2.0 seconds. Table 4.1 shows the setup for this experiment. Figure 4.9 is the location of the SC unit in the wave flume. The value from this experiment will then be plotted into two graphs:

1. Graph of Transmission Coefficient, K_t versus Wave Period, T
2. Graph of Transmission Coefficient, K_t versus Wave Steepness, H/gT^2

Table 4.1: Experimental Setup for Third Experiment

Arrangement			Water Depth (d), cm	Wave Period (T), s
Figure	Base Width (B), cm	Height (h), cm		
	10	6.5	10	0.6
	20	6.5		1.0
	30	6.5		1.3
	40	6.5		1.6
				2.0

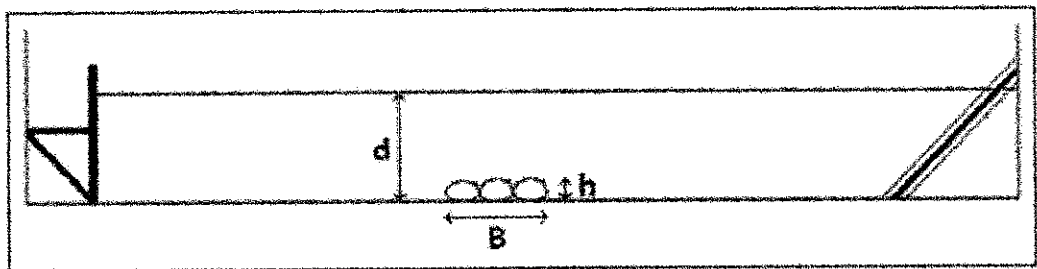


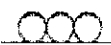
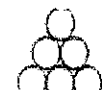
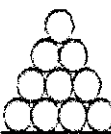
Figure 4.9: SC Unit Location in Wave Flume for Third Experiment

4.3.4. Water Depth, d , Freeboard, f and Structure Height, h Effect Towards Transmission Coefficient, K_t

This experiment is carried out to determine the transmission coefficient (K_t) for different structure arrangements and different water depths by using five (5) wave periods for each scenario. This is done by determine the transmission wave height, (H_t) for each scenario and divide by the respective incident wave height (H_i) that has been determined in the second experiment. The wave periods used are 0.6 s, 1.0 s, 1.3 s, 1.6 s and 2.0 s.

The experimental setup used for each scenario is summarised in Table 4.2. Figure 4.10 is the configurations of the SCU in the wave flume.

Table 4.2: Experimental Setup for Fourth Experiment

Configuration		Arrangement		Water Depth (d), cm	Wave Period (T), s
		Base Width (B), cm	Height (h), cm		
1		30	6.5	8	0.6
				12	1.0
				16	1.3
				20	1.6
				20	2.0
2		30	13	15	0.6
				18	1.0
				20	1.3
				22	1.6
				24	2.0
3		30	19.5	22	0.6
				24	1.0
				26	1.3
				28	1.6
				28	2.0
4		40	26	26	0.6
				28	1.0
				30	1.3
				30	1.6
				32	2.0

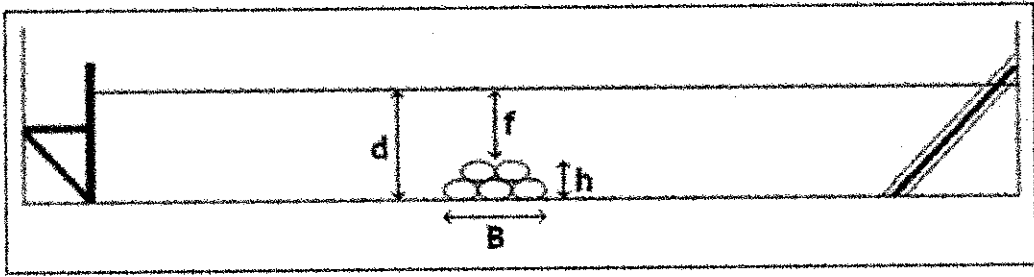


Figure 4.10: SC Unit Location in Wave Flume for Fourth Experiment

Results obtained from this experiment will be plotted as follow:

1. Graph of Transmission Coefficient, K_t versus Wave Period, T
2. Graph of Transmission Coefficient, K_t versus f/d
3. Graph of Transmission Coefficient, K_t versus d/gT^2

CHAPTER 5

RESULTS AND DISCUSSION

5.1. INTRODUCTION

In this chapter, all the results of the experiments and findings is presented for both two phases of this study. Two experiments were conducted during the first phase which focused on calibrating the wave flume device and determining the incident wave height (H_i). Second phase of study also involved two experiments. The first experiment was to determine transmission coefficient (K_t) for given base width (B) by using five (5) wave periods for each scenario. Second experiment was carried out to determine the transmission coefficient (K_t) for different structure arrangements and different water depths by using five (5) wave periods for each scenario. Both were done by determining the transmission wave height (H_t) and using the formula discussed in Chapter 2. From Chapter 2, transmission coefficient (K_t), is depends on three major factors (see Equation 5);

$$K_t = \frac{H_t}{H_i} = f \left[\frac{H_i}{gT^2}, \frac{h}{d}, \frac{h}{B} \right] \quad \text{Equation 5}$$

5.2. FREQUENCY VERSUS WAVE PERIOD

Wave period (T) is defined as the time for a successive wave to pass a given point. However, in this laboratory experiment, the wave period is determined by measuring the time taken for the crank disk to make one complete rotation. This is because the one crank disk rotation will generate one successive wave formation. Table 5.1 shows the result from the experiment. Figure 5.1 is the generated graph for the experiment.

Table 5.1: Wave Period, T for Various Frequencies, Hz

Frequency, f (Hz)	Wave Period, T (s)			
	1	2	3	Average
20	4.50	4.49	4.49	4.50
25	3.13	3.12	3.11	3.12
30	2.38	2.39	2.37	2.38
35	1.92	1.91	1.91	1.91
40	1.61	1.62	1.62	1.62
45	1.38	1.38	1.38	1.38
50	1.00	1.00	1.01	1.01
55	0.91	0.89	0.91	0.90
60	0.83	0.83	0.83	0.83
65	0.76	0.76	0.77	0.76
70	0.70	0.69	0.71	0.70
75	0.65	0.65	0.65	0.65
80	0.61	0.60	0.60	0.60
85	0.55	0.54	0.58	0.56
90	0.52	0.52	0.52	0.52
95	0.50	0.49	0.50	0.49
100	0.49	0.49	0.49	0.49

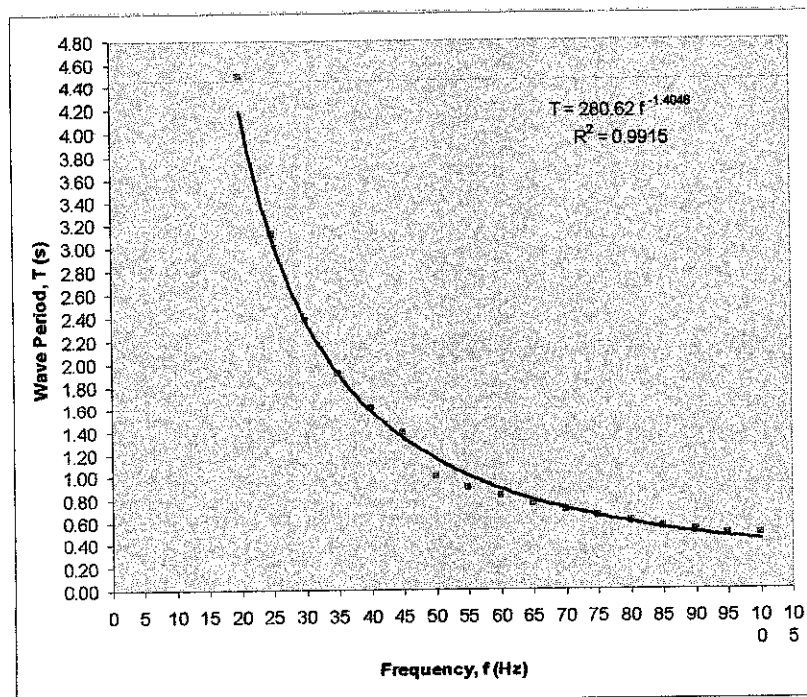


Figure 5.1: Wave Period, T versus Frequency, Hz Graph

The graph above shows that the wave period, T is decreases exponentially with the increasing of frequency. The determined relationship formula (self generated by using Microsoft Excel) is used to determine the stroke frequency of the potentiometer for a set of wave period. The relationship is given by:

$$T = 280.62 f^{-1.4046} \quad \text{Equation 6}$$

This equation is very important in determining the actual stroke frequency for the respective wave period. Table 5.2 shows the values of each frequency for the given wave period.

Table 5.2: Corresponding Stroke Frequency, Hz versus Wave Period, T

Wave Period (s)	Stroke Frequency, (Hz)
0.5	90.62
0.6	79.59
0.7	71.32
0.8	64.85
0.9	59.64
1.0	55.33
1.1	51.70
1.2	48.59
1.3	45.90
1.4	43.54
1.5	41.45
1.6	39.59
1.7	37.92
1.8	36.41
1.9	35.03
2.0	33.78

5.3. WAVE PERIOD (T) VERSUS INCIDENT WAVE HEIGHT (H_i)

Incident wave height (H_i) is the height of wave approaching the tested modelled structure. It is measured at the section prior to the placement of the model. The incident wave height will be used in determining the wave transmission coefficient (K_t) in the third and fourth experiments. Table 5.3 shows the final result of the experiment and Figure 5.2 shows the corresponding graph.

Table 5.3: Corresponding Incident Wave Height, H_i versus Wave Period, T

Wave Period, T	Water Depth, d												
	8	10	12	15	16	18	20	22	24	26	28	30	32
0.6	3.00	3.30	3.70	3.87	4.25	4.30	4.45	4.93	5.17	5.50	5.34	4.89	4.50
1.0	2.15	2.70	3.42	4.27	5.30	6.21	7.50	8.03	8.73	9.50	10.23	10.78	11.10
1.3	1.60	2.13	2.45	3.67	4.12	4.67	6.00	6.83	7.63	8.20	8.45	9.25	10.00
1.6	1.15	1.67	2.00	2.84	3.29	3.87	4.56	5.00	5.64	6.00	6.50	6.90	7.40
2.0	1.00	1.43	1.75	2.20	2.53	3.15	3.53	4.43	4.93	5.32	5.64	5.50	5.20

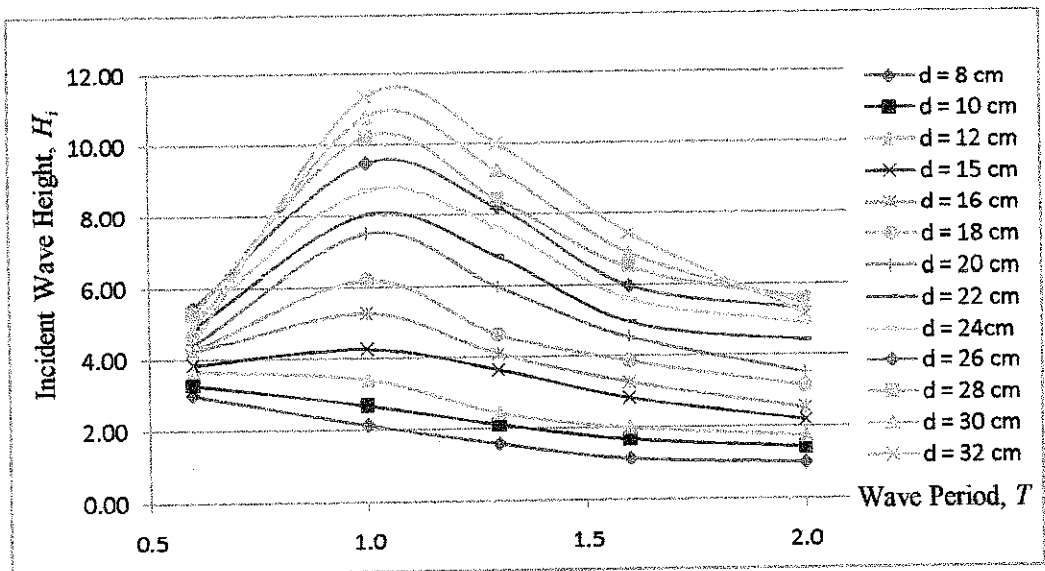


Figure 5.2: Incident Wave Height, H_i versus Wave Period, T

From Figure 5.2, it is clearly seen that the trend of the incident wave height, H_i is highly dependent to wave period, T with the respective water depth, d for wave period, T of 0.6, 1.0, 1.3, 1.6 and 2.0 s.

For water depth 8, 10 and 12 cm, incident wave height, H_i is decreases by the increasing of wave period, T . The decreases pattern however is very gradual for wave period, T from 0.6 s to 1.0 s and 1.6 s to 2.0 s. For wave period, T of 1.0 s and 1.6 s, more obvious decreases of incident wave height, H_i are observed. The peaks of the incident wave height, H_i are 3.00, 3.30 and 3.70 cm respectively.

For 15, 16 and 18 cm water depth, d the initial wave height, H_i trend started to change where incident wave height, H_i are initially increases until reaches peak and then decreases. Incident wave height, H_i trend increases for wave period, T from 0.6 s to 1.0 s and having peak of 4.24, 5.30, and 6.21 cm respectively at wave period, T of 1.0 s. However, the trend starts to decreases gradually from 1.0 s to 2.0 s.

For water depth, d of 20, 22, 24 and 26 cm, the incident wave height, H_i trend is similar for 15, 16 and 18 cm water depth, d but the initial increases are more likely rapid and having quite high peak value (at wave period, T of 0.6 s to 1.0 s). The peaks recorded are 7.50, 8.03, 8.73, and 9.50 cm respectively. The incident wave height, H_i decreases more severely compared to the previous water depths, d record at wave period, T of 1.0 s to 1.6 s. However, gradual decreases are observed for wave period, T from 1.6 s to 2.0 s.

For water depth, d of 28, 30 and 32 cm, the incident wave height, H_i trend changes extremely. Exponential increases are observed from wave period, T 0.6 s to 1.0 s. Then, incident wave height, H_i decreases drastically from wave period, T 1.0 s to 2.0 s. Also from the experiment, the incident wave height, H_i is decreases for wave period, T 0.6 s and 2.0 s with the increases of water depth, d . The peaks recorded are 10.30, 10.90 and 11.50 cm respectively.

Based on all these observation, it is concluded that the incident wave height, H_i is dependent on the wave period, T . This result is actually unique and will depend on the wave flume used. Different wave flume will usually generate different value of incident wave height (H_i)

5.4. BASE WIDTH, b AND WAVE STEEPNESS, H/gT^2 EFFECT TOWARDS TRANSMISSION COEFFICIENT, K_T

Transmission coefficient, K_t for given base width is determined by dividing transmission wave height, H_t and incident wave height, H_i . This dimensionless parameter will be used throughout this study and is representing the wave attenuation of the system. As previously described in chapter 2, transmission coefficient, K_t is given by:

$$K_t = \frac{H_t}{H_i}$$

The incident wave height (H_i) was determined from the second experiment and thus, the value of transmission wave height (H_t) need to be determined in this experiment.

For this experiment, the results are presented in two graphs. First graph (Figure 5.3) is plotted to be transmission coefficient, K_t versus wave period, T . This graph will show the relationship between transmission coefficient, K_t and wave period, T . While for the second graph (Figure 5.4), transmission coefficient, K_t is plotted versus wave steepness, H/gT^2 . This graph will show the relationship between transmission coefficient, K_t and wave steepness, H/gT^2 .

5.4.1. Graph of Transmission Coefficient, K_t versus Wave Period, T

Table 5.4 below shows the result for this third experiment. The value is then plotted into graph as shown in figure 5.3.

Table 5.4: Transmission Coefficient, K_t for Corresponding Wave Period, T for Four Dimensionless Base Widths, h/B .

T	h/B			
	0.650	0.325	0.217	0.163
0.6	0.72	0.64	0.45	0.39
1.0	0.73	0.66	0.49	0.43
1.3	0.75	0.68	0.54	0.46
1.6	0.77	0.71	0.60	0.51
2.0	0.80	0.75	0.67	0.57

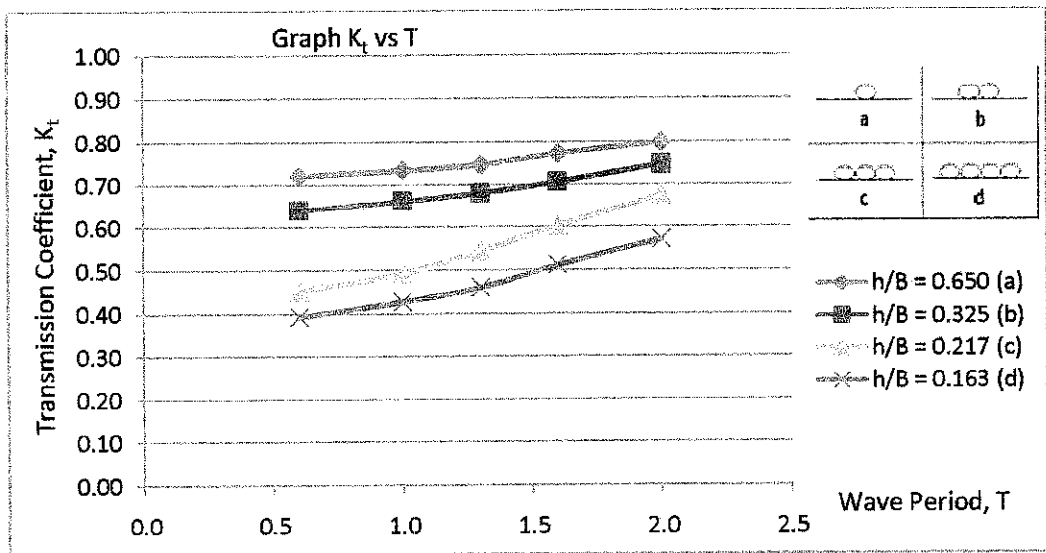


Figure 5.3: Transmission Coefficient, K_t for Corresponding Wave Period, T for Four Base Widths, B .

From the results above, it is observed that the transmission coefficient, K_t , increases with the increasing of wave period, T . Besides, transmission coefficient, K_t , also increases with the increasing of h/B .

The sudden change in water depth tends the wave to breaks on the structure. Wave that breaks will decapitate the energy throughout the system (water) where some of the energy change to sound energy, and some are reflected back to the source. Longer base will have more waves tend to breaks, thus more energy is dissipated.

5.4.2. Graph of Transmission Coefficient, K_t , versus Wave Steepness, H_i/gT^2

For the second graphs, Table 5.5 below shows the respective value for the graph.

Table 5.5: Transmission Coefficient, K_t , for Corresponding Wave Steepness, H_i/gT^2 for Four Dimensionless Base Widths, h/B .

T, s	H_i , cm	H_i/gT^2	h/B			
			0.650	0.325	0.217	0.163
0.6	3.30	9.34×10^{-4}	0.72	0.64	0.45	0.39
1.0	2.75	2.80×10^{-4}	0.73	0.66	0.49	0.43
1.3	2.57	1.55×10^{-4}	0.75	0.68	0.54	0.46
1.6	2.17	0.86×10^{-4}	0.77	0.71	0.60	0.51
2.0	2.70	0.69×10^{-4}	0.80	0.75	0.67	0.57

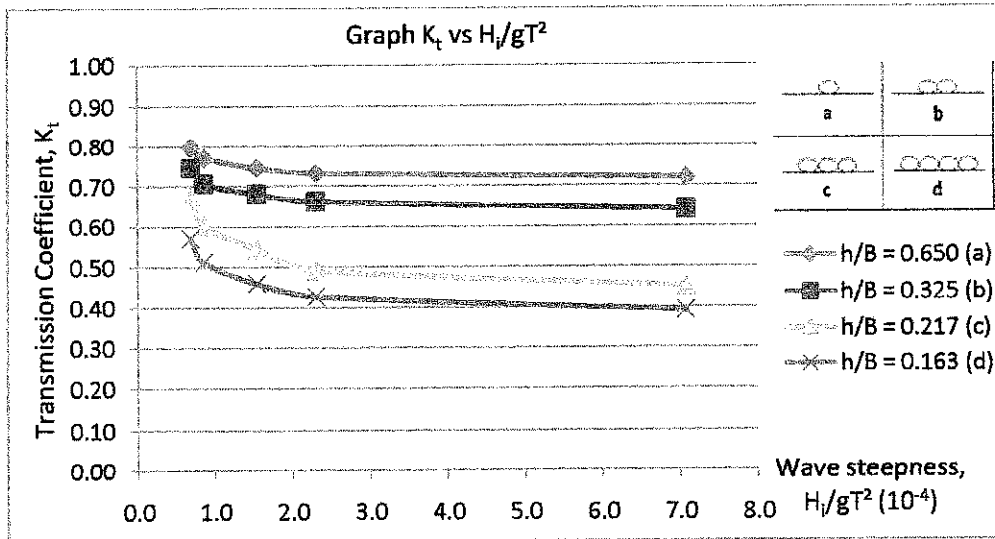


Figure 5.4: Transmission Coefficient, K_t for Corresponding Wave Period, T for Four Base Widths, B .

From the graphs, observed that the transmission coefficient, K_t decreases with the increasing of wave steepness, H_i/gT^2 . Sudden decrease of transmission coefficient, K_t is observed for wave steepness, H_i/gT^2 from 0.00069 to 0.0086. The decreases for wave steepness, H_i/gT^2 from 0.00089 to 0.000934 are gradual and consistence. The graph also shows that the transmission coefficient, K_t increases with the increasing of h/B .

The relationship of the transmission coefficient, K_t and h/B indicates that the system will attenuate more energy when the system is having longer base width, B (as h is constant throughout the experiment).

From both graphs from Figure 5.3 and 5.4, the transmission coefficient trend clearly showed that it will increase with the increasing of wave period, T , increase with the increasing of base width, B , and decrease with the increasing of wave steepness, H_i/gT^2 .

5.5. WATER DEPTH, d , FREEBOARD, f , AND STRUCTURE HEIGHT, h , EFFECT TOWARDS TRANSMISSION COEFFICIENT, K_t

There are four different configurations of sand container used in this experiment. For each configuration, there will be three (3) different graphs plotted to shows the relationship of the transmission coefficient, K_t to the respective parameters.

5.5.1. Graph of Transmission Coefficient, K_t versus Wave Period, T

This graph shows the relationship between transmission coefficient, K_t , and wave period, T . Besides, relationship between transmission coefficient, K_t , and water depth, d , also can be determined. Table 5.6, 5.7, 5.8 and 5.9 shows the result for the respective configurations and Figure 5.5, 5.6, 5.7 and 5.8 are the plotted graphs from the respective tables.

Table 5.6: Transmission Coefficient, K_t for Corresponding Wave Period, T , for $h/B = 0.217$

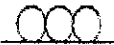
Configuration	Wave Period, T	Water Depth, cm			
		8	12	16	20
	0.6	0.30	0.47	0.55	0.63
	1.0	0.42	0.52	0.59	0.68
	1.3	0.50	0.57	0.68	0.75
	1.6	0.56	0.65	0.77	0.85
	2.0	0.65	0.74	0.85	0.96

Table 5.7: Transmission Coefficient, K_t , for Corresponding Wave Period, T , for h/B
 $= 0.430$

Configuration	Wave Period, T	Water Depth, cm				
		15	18	20	22	24
	0.6	0.31	0.41	0.58	0.78	0.85
	1.0	0.36	0.48	0.64	0.82	0.87
	1.3	0.41	0.53	0.71	0.86	0.90
	1.6	0.45	0.57	0.75	0.89	0.94
	2.0	0.52	0.63	0.81	0.93	0.97

Table 5.8: Transmission Coefficient, K_t , for Corresponding Wave Period, T , for h/B
 $= 0.650$ (a)

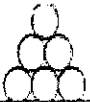
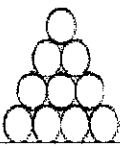
Configuration	Wave Period, T	Water Depth, cm			
		22	24	26	28
	0.6	0.40	0.46	0.49	0.59
	1.0	0.45	0.54	0.64	0.66
	1.3	0.50	0.57	0.70	0.78
	1.6	0.60	0.65	0.73	0.80
	2.0	0.72	0.75	0.89	0.92

Table 5.9: Transmission Coefficient, K_t , for Corresponding Wave Period, T , for h/B
 $= 0.650$ (b)

Configuration	Wave Period, T	Water Depth, cm			
		26	28	30	32
	0.6	0.25	0.31	0.48	0.56
	1.0	0.31	0.35	0.51	0.58
	1.3	0.35	0.43	0.54	0.64
	1.6	0.40	0.49	0.64	0.68
	2.0	0.53	0.56	0.78	0.88

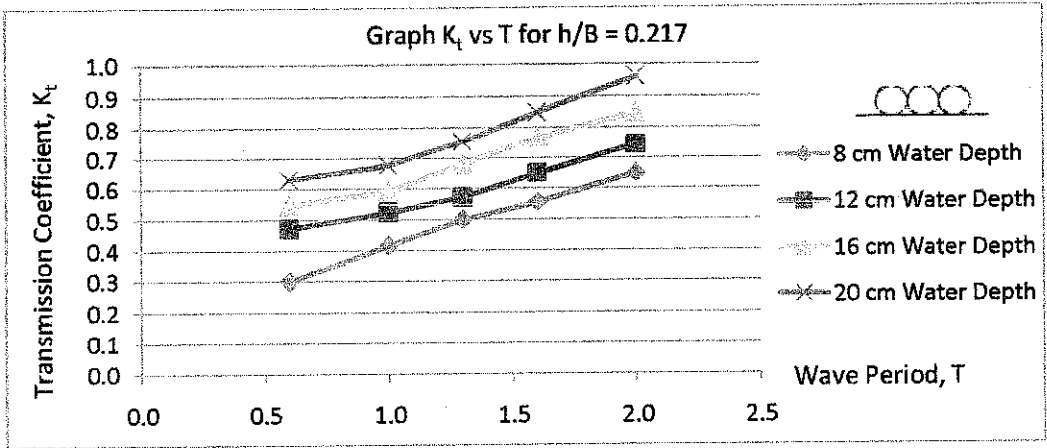


Figure 5.5: Transmission Coefficient, K_t , for Corresponding Wave Period, T for $h/B = 0.217$

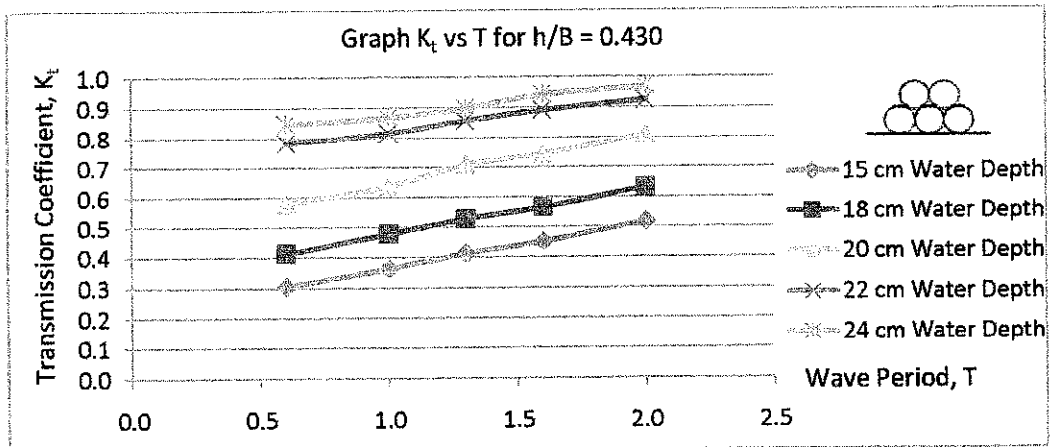


Figure 5.6: Transmission Coefficient, K_t , for Corresponding Wave Period, T for $h/B = 0.430$

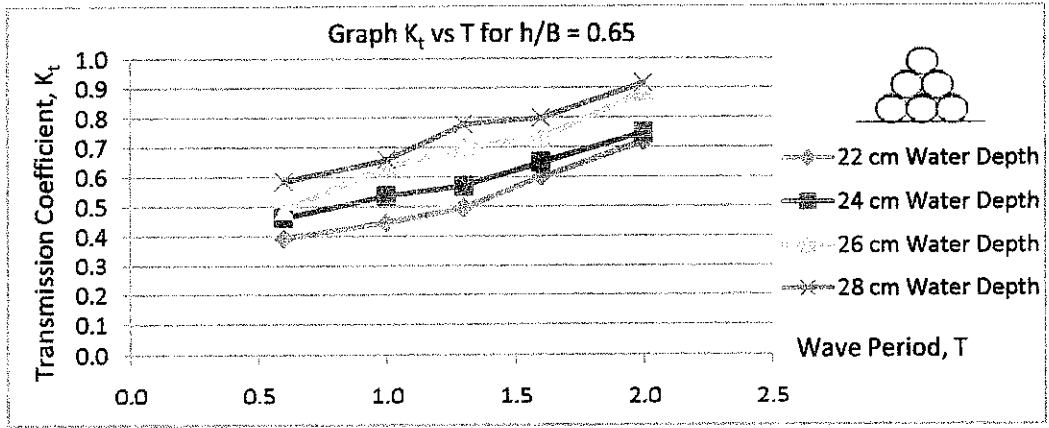


Figure 5.7: Transmission Coefficient, K_t , for Corresponding Wave Period, T for $h/B = 0.650$ (a)

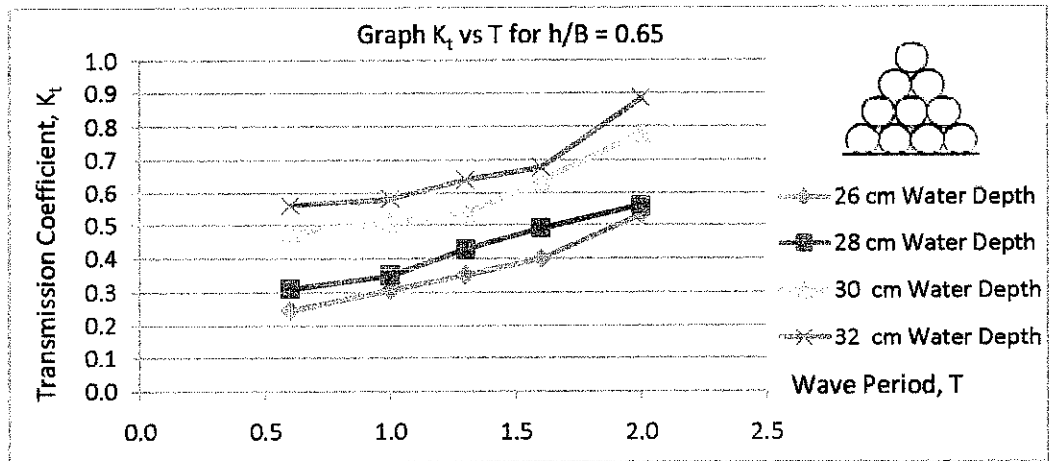


Figure 5.8: Transmission Coefficient, K_t , for Corresponding Wave Period, T for $h/B = 0.650$ (b)

From Figure 5.5, 5.6, 5.7 and 5.8, it is observed that all graphs plotted has similar trend where the transmission coefficient, K_t , increases with the increasing of wave period, T . Besides, the higher the water depth, d , the higher the transmission coefficient, K_t . The increment of transmission coefficient, K_t , for configuration 1 and 2 is quite constant with the increasing of wave period, T compared that for configuration 3 and 4. Configuration 3 and 4 are having the same h/B (0.650), but

observed that configuration 4 recorded smaller value of transmission coefficient, K_t (for water depth, d 26 and 28 cm). This behaviour however cannot be explained using this graph, thus, second series of graphs is plotted for transmission coefficient, K_t versus f/d (f is the freeboard and d is the water depth).

5.5.2. Graph of Transmission Coefficient, K_t versus f/d

Relationship between transmission coefficient and f/d is determined from this section. Table 5.10, 5.11, 5.12 and 5.13 show the result for the respective configurations and Figure 5.9, 5.10, 5.11 and 5.12 are the plotted graphs from the respective tables.

Table 5.10: Transmission Coefficient, K_b , for Corresponding f/d , for $h/B = 0.217$

Configuration	Wave Period, T	f/d			
		0.188	0.458	0.594	0.675
	0.6	0.30	0.47	0.55	0.63
	1.0	0.42	0.52	0.59	0.68
	1.3	0.50	0.57	0.68	0.75
	1.6	0.56	0.65	0.77	0.85
	2.0	0.65	0.74	0.85	0.96

Table 5.11: Transmission Coefficient, K_b , for Corresponding f/d , for $h/B = 0.430$

Configuration	Wave Period, T	f/d				
		0.133	0.278	0.350	0.409	0.458
	0.6	0.31	0.41	0.58	0.78	0.85
	1.0	0.36	0.48	0.64	0.82	0.87
	1.3	0.41	0.53	0.71	0.86	0.90
	1.6	0.45	0.57	0.75	0.89	0.94
	2.0	0.52	0.63	0.81	0.93	0.97

Table 5.12: Transmission Coefficient, K_t , for Corresponding f/d , for $h/B = 0.650$ (a)

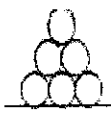
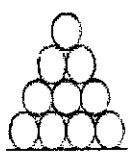
Configuration	Wave Period, T	f/d			
		0.114	0.188	0.250	0.304
	0.6	0.40	0.46	0.49	0.59
	1.0	0.45	0.54	0.64	0.66
	1.3	0.50	0.57	0.70	0.78
	1.6	0.60	0.65	0.73	0.80
	2.0	0.72	0.75	0.89	0.92

Table 5.13: Transmission Coefficient, K_t , for Corresponding f/d , for $h/B = 0.650$ (b)

Configuration	Wave Period, T	f/d			
		0.000	0.071	0.133	0.188
	0.6	0.25	0.31	0.48	0.56
	1.0	0.31	0.35	0.51	0.58
	1.3	0.35	0.43	0.54	0.64
	1.6	0.40	0.49	0.64	0.68
	2.0	0.53	0.56	0.78	0.88

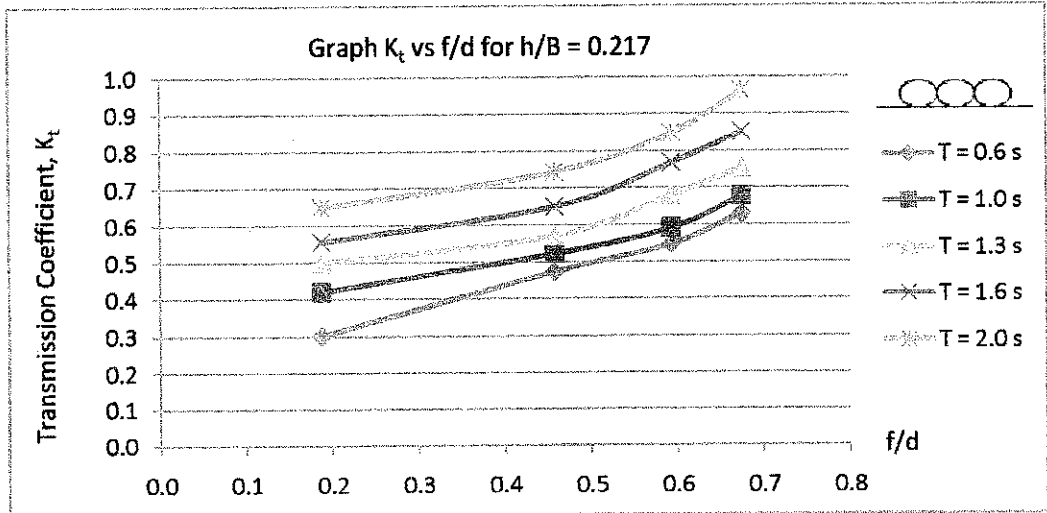


Figure 5.9: Transmission Coefficient, K_t , for Corresponding f/d for $h/B = 0.217$

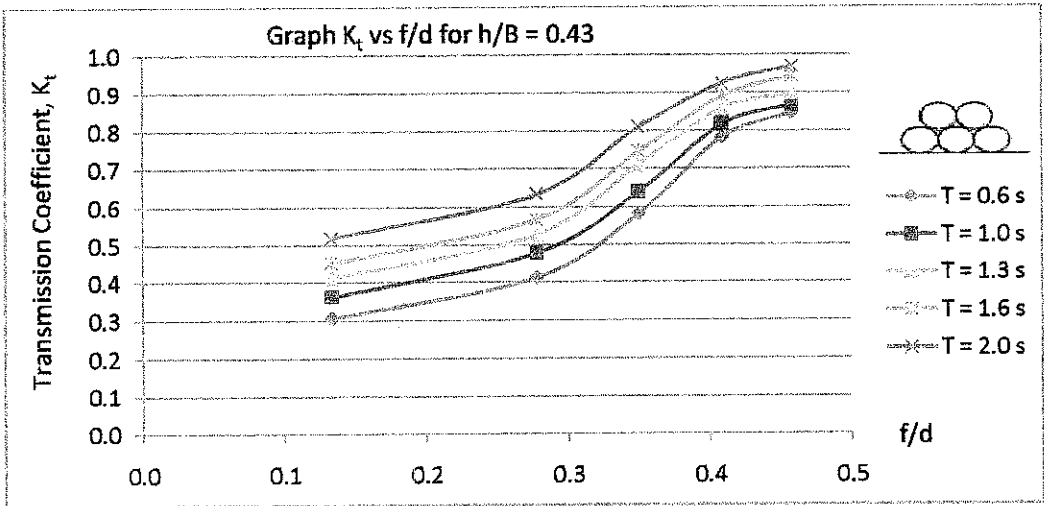


Figure 5.10: Transmission Coefficient, K_t for Corresponding f/d , for $h/B = 0.430$

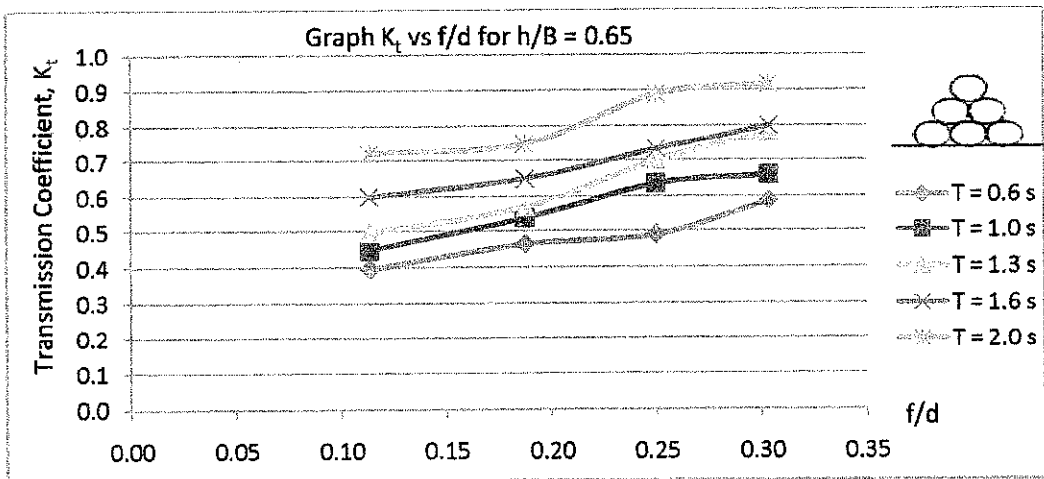


Figure 5.11: Transmission Coefficient, K_t for Corresponding f/d , for $h/B = 0.650$ (a)

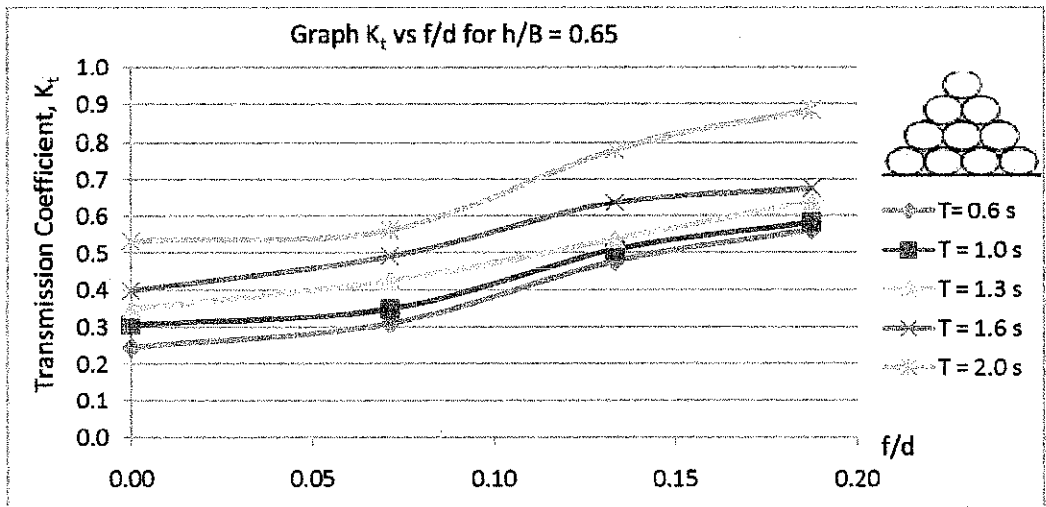


Figure 5.12: Transmission Coefficient, K_t for Corresponding f/d , for $h/B = 0.650$ (b)

Figure 5.9, 5.10, 5.11 and 5.12 show that transmission coefficient, K_t is increases with the increasing of f/d . For a given h/B , the only parameter that changes is the freeboard, f , where the deeper the depth, d , the higher the freeboard, f . Thus, increasing the freeboard, f will increases the transmission coefficient, K_t . The graphs also show that transmission coefficient, K_t increases with the increasing of wave period, T (as previously shown before), and the transmission coefficient, K_t decreases with the increasing of structure height, h . During this experiment, for small freeboard, f system, waves were almost immediately broken after the crest, and vice-versa (see Figure 5.13 and 5.14). This wave breaking phenomenon will distribute the wave energy throughout the system.

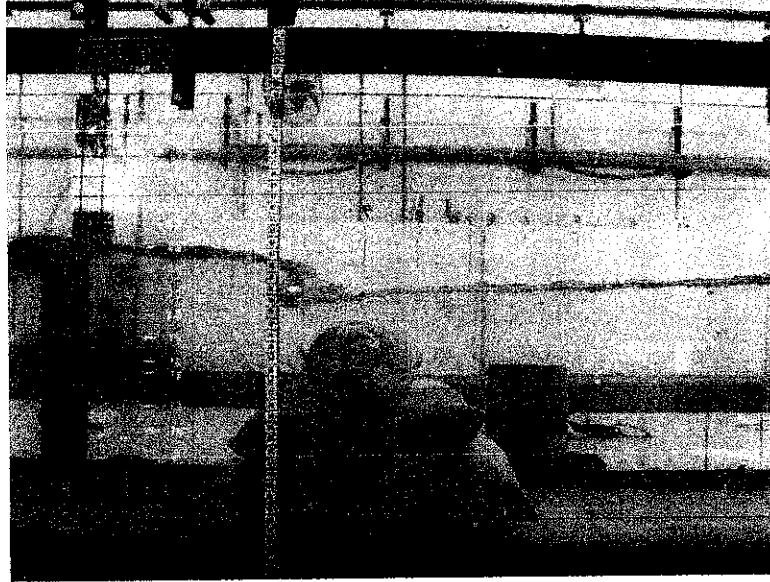


Figure 5.13: Wave breaking at wave period, $T = 2.0$ s, freeboard $f = 1.5$ cm

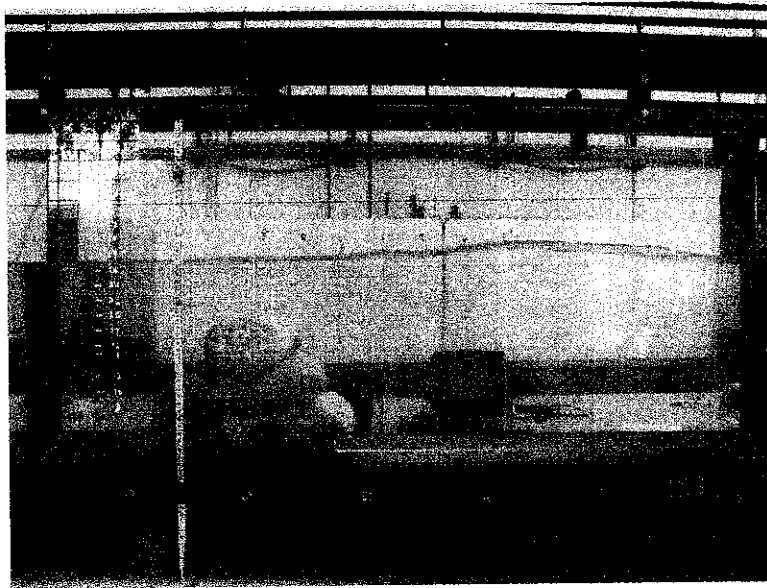


Figure 5.14: No obvious wave breaking at wave period, $T = 2.0$ s, freeboard, $f = 7.5$ cm

5.5.3. Graph of Transmission Coefficient, K_t , versus d/gT^2

Table 5.14, 5.15, 5.16 and 5.17 shows the result for the respective configurations and Figure 5.15, 5.16, 5.17 and 5.18 are the plotted graphs from the respective tables.

Table 5.14: Transmission Coefficient, K_t , for Corresponding d/gT^2 , for $h/B = 0.217$

Configuration	Wave Period, T	Water Depth, cm							
		8		12		16		20	
		d/gT^2	K_t	d/gT^2	K_t	d/gT^2	K_t	d/gT^2	K_t
	0.6	2.265	0.30	3.398	0.47	4.531	0.55	5.663	0.63
	1.0	0.815	0.42	1.223	0.52	1.631	0.59	2.039	0.68
	1.3	0.483	0.50	0.724	0.57	0.965	0.68	1.206	0.75
	1.6	0.319	0.56	0.478	0.65	0.637	0.77	0.796	0.85
	2.0	0.204	0.65	0.306	0.74	0.408	0.85	0.510	0.96

Table 5.15: Transmission Coefficient, K_t , for Corresponding d/gT^2 , for $h/B = 0.430$

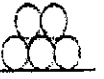
Configuration	Wave Period, T	Water Depth, cm									
		15		18		20		22		24	
		d/gT^2	K_t	d/gT^2	K_t	d/gT^2	K_t	d/gT^2	K_t	d/gT^2	K_t
	0.6	4.247	0.31	5.097	0.41	5.663	0.58	6.229	0.78	6.796	0.8
	1.0	1.529	0.36	1.835	0.48	2.039	0.64	2.243	0.82	2.446	0.8
	1.3	0.905	0.41	1.086	0.53	1.206	0.71	1.327	0.86	1.448	0.9
	1.6	0.597	0.45	0.717	0.57	0.796	0.75	0.876	0.89	0.956	0.9
	2.0	0.382	0.52	0.459	0.63	0.510	0.81	0.561	0.93	0.612	0.9

Table 5.16: Transmission Coefficient, K_t , for Corresponding d/gT^2 , for $h/B = 0.650$

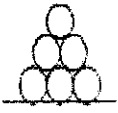
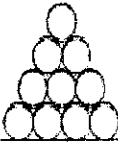
Configuration	Wave Period, T	Water Depth, cm							
		22		24		26		28	
		d/gT^2	K_t	d/gT^2	K_t	d/gT^2	K_t	d/gT^2	K_t
	0.6	6.229	0.40	6.796	0.46	7.362	0.49	7.928	0.59
	1.0	2.243	0.45	2.446	0.54	2.650	0.64	2.854	0.66
	1.3	1.327	0.50	1.448	0.57	1.568	0.70	1.689	0.78
	1.6	0.876	0.60	0.956	0.65	1.035	0.73	1.115	0.80
	2.0	0.561	0.72	0.612	0.75	0.663	0.89	0.714	0.92

Table 5.17: Transmission Coefficient, K_t , for Corresponding d/gT^2 , for $h/B = 0.650$

Configuration	Wave Period, T	Water Depth, cm							
		26		28		30		32	
		d/gT^2	K_t	d/gT^2	K_t	d/gT^2	K_t	d/gT^2	K_t
	0.6	7.362	0.25	7.928	0.31	8.495	0.48	9.061	0.56
	1.0	2.650	0.31	2.854	0.35	3.058	0.51	3.262	0.58
	1.3	1.568	0.35	1.689	0.43	1.810	0.54	1.930	0.64
	1.6	1.035	0.40	1.115	0.49	1.195	0.64	1.274	0.68
	2.0	0.663	0.53	0.714	0.56	0.765	0.78	0.815	0.88

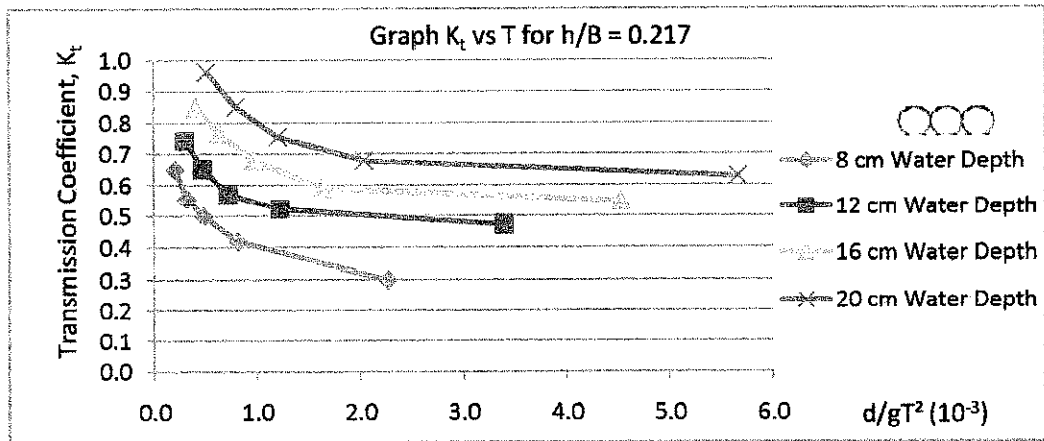


Figure 5.15: Transmission Coefficient, K_t , for Corresponding d/gT^2 , for $h/B = 0.217$

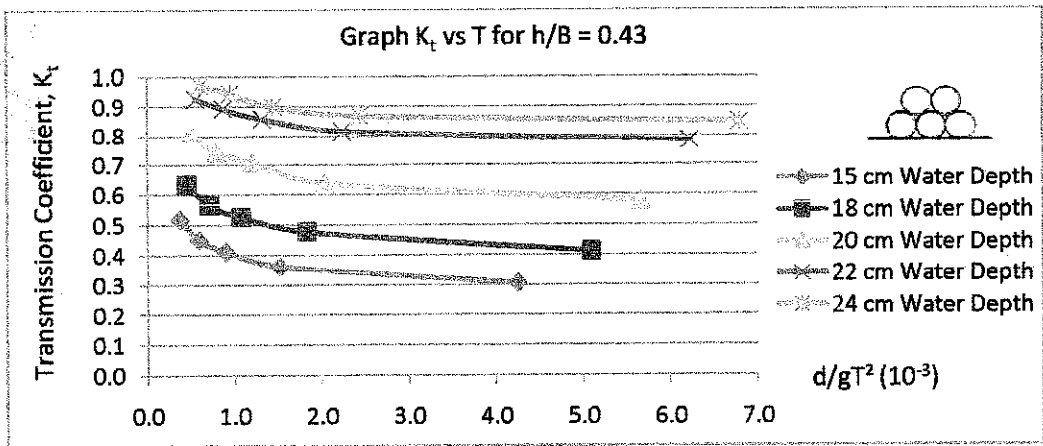


Figure 5.16: Transmission Coefficient, K_t for Corresponding d/gT^2 , for $h/B = 0.430$

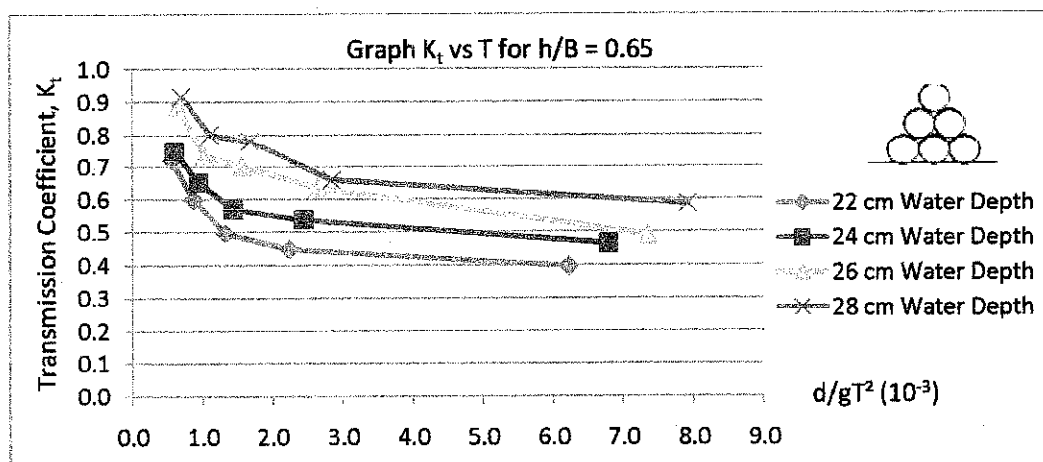


Figure 5.17: Transmission Coefficient, K_t for Corresponding d/gT^2 , for $h/B = 0.650$

(a)

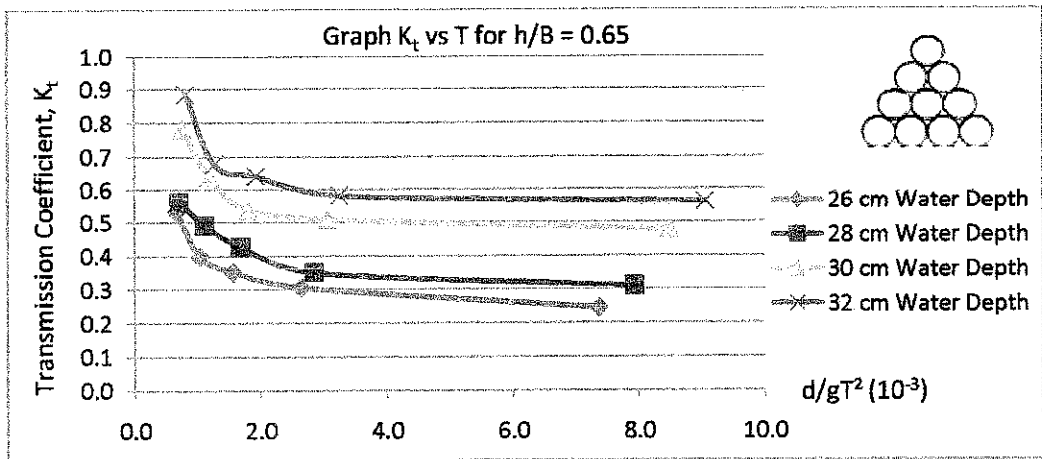


Figure 5.18: Transmission Coefficient, K_t for Corresponding d/gT^2 , for $h/B = 0.650$
(b)

From Figure 5.15, 5.16, 5.17 and 5.18, transmission coefficient, K_t is decreases with the increasing of d/gT^2 . Referring to these plotted graphs, for the same value of d/gT^2 in any graphs, the transmission coefficient, K_t is increases with the increasing of water depth, d . The trends of these graphs however very differ compared to other graphs previously discussed.

Rapid decrease in transmission coefficient, K_t is observed at the initial stage of these graphs before it reach a point where the graph started to decrease gradually (almost constant). This behaviour shows that the transmission coefficient is severely affected by d/gT^2 at the certain initial points only and it started to not affected by the increasing of the d/gT^2 .

Comparing graph in Figure 5.17 and 5.18, for $d/gT^2 = 2.0$, and water depth, $d = 26$ and 28 cm, the transmission coefficient, K_t for configuration 4 is higher than that recorded for configuration 3. This again is because of the freeboard, f different between the two configurations.

CHAPTER 6

CONCLUSION AND RECOMMENDATION

6.1. CONCLUSION

This study is performed to observe the wave attenuation characteristic of the sand container. After doing extensive literature review on the related materials, it is understood that this new technologies has performed very well as a replacing material for conventional materials (rock, steel etc). Most of the responses received were that this new invention can shorten the construction period, reliable, and cost effective. This system has save the well-known tourism area in Narrowneck, Australia. Besides, this less-permanent structure is very flexible and can well replace any other permanent structure of its kind.

The second objective was to develop a small scale model of sand container. From the literature review, many projects that use this material applied cylindrical-shape sand container. However, the size and length of the sand container can be varies depending on the project and the nature of the location. However, for a small sand container, the commonly design diameter is about 1 meter. For the purpose of this study, a small scale model of sand container has been constructed using cotton fabric with the cylindrical dimension of 8 cm diameter and 30 cm length.

The sand container is only filled until 80-85% of the volume (as reviewed from the literature review). After the completion of the model, the final shape is an ellipse-like sand container with height, h of 10 cm and base width, B of 6.5 cm. The scale down model is 1:12.5 (as 8 cm to 100 cm of diameter). The laboratory wave flume can only generated a 2-D waves, thus the length of the system can be neglected (and as in real construction, the length also can be very varies).

The second objective is to study the performance of the proposed sand containers via hydraulic model simulation in laboratory. There are total of ten (10) sand container unit (SCU) used in the experiment. Total of four (4) experiments have

been carried out where two of them were during the first phase of the study and another two were during this second phase of study. First experiment is very important as to make sure that all the equipments and instruments are available and ready to be used. This experiment is done to calibrate these equipments and instruments and determine the relationship between the wave period (T) and stroke frequency (Hz). This experiment concluded that the relationship is:

$$T = 280.62 f^{-1.4046} \quad \text{where } T = \text{Wave period}$$

$$F = \text{Stroke frequency}$$

After calibrating the wave flume system, the small scale sand containers are ready to be tested. In this experiment, the transmission coefficient, K_t is determined using different configurations of SCU and wave period, T . As stated in Chapter 2, transmission coefficient, K_t is given by;

$$K_t = \frac{H_t}{H_i} = f \left[\frac{H_i}{gT^2}, \frac{h}{d}, \frac{h}{B} \right]$$

Based on the above function, the value of incident wave height, H_i is determined during the second experiment. This experiment was done successfully and the incident wave height, H_i results is as shown in Figure 5.2.

The second half of this study is the most crucial part of this study. As the value of incident wave height, H_i has been determine, the second half will be to determine the transmission coefficient, K_t value by determining the transmission wave height, H_t of the system.

Thus, come the third experiment was tool place in the early of the second phase of this study. The relationship between the transmission coefficient, K_t and the base width, B and wave steepness, H_i/gT^2 of the structure has been determined. The graphs plotted in Figure 5.3 and 5.4 conclude that:

1. Transmission coefficient, K_t increases with the increasing of wave period, T .
2. Transmission coefficient, K_t increases with the increasing of base width, B .
3. Transmission coefficient, K_t decreases with the increasing of wave steepness, H/gT^2 .

The fourth experiment is conducted to find the relationship between transmission coefficient, K_t with the water depth, d , freeboard, f , and structure height, h . From Figure 5.5 to Figure 5.16, it is concluded that:

1. Transmission coefficient, K_t increases with the increasing of water depth, d .
2. Transmission coefficient, K_t increases with the increasing of f/d .
3. Transmission coefficient, K_t increases with the increasing the freeboard, f .
4. Transmission coefficient, K_t is decreases with the increasing of structure height, h .
5. Transmission coefficient, K_t is decreases with the increasing of d/gT^2 .

Thus, concluded that the wave attenuation of sand container is depend on those above parameter and thus to have the optimum performance of the sand container, all of the above parameters must be considered.

As far as a submerged breakwater is concern, the best configuration will be the configuration that will give the smallest transmission coefficient, K_t . In this study, the smallest value of transmission coefficient is 0.31 with the configuration of:

1. Wave Period, $T = 0.6$ s
2. Base Width, $B = 40$ cm
3. Water Depth, $d = 28$ cm
4. Structure Height, $h = 26$ cm
5. Freeboard, $f = 2$ cm

Thus, the highest value of transmission coefficient, K_t will be the worst or ineffective to be designed for submerged breakwater. From the overall graphs generated, the highest value of transmission coefficient, K_t recorded is 0.97 when the configuration where:

1. Wave Period, $T = 2.0$ s
2. Base Width, $B = 30$ cm
3. Water Depth, $d = 24$ cm
4. Structure Height, $h = 13$ cm
5. Freeboard, $f = 11$ cm

6.2. RECOMMENDATION

During the experimenting process, it is observed that the waves were not perfectly generated where two different wave lengths were observed in the wave flume at a time. With two waves observed in the wave flume, it is quite hard to get the best value of incident wave height, H_i , and transmission wave height, H_t . This formed probably because of the wave absorber system used was not efficient to absorb the wave energy and thus some of the wave energy was reflected. Thus, below are some recommendations to this problem.

1. To reduce the effect, it is advised to take the wave height reading at the first five to ten second after the system started generating the waves.
2. Error in reading also can be minimise if level gauge device is use to take the reading.

As this study is completed, it is found that this sand container is an interesting new technology, which proven to be effectively attenuate waves. Thus, as far as this study is concern, more study can be made to further understand this sand container characteristics. Study can be made on:

1. Designing and testing new model of sand container.
2. Studying the effects of sand bag porosity towards the wave attenuation.

REFERENCES

Azmi, A. H., Assistant Director, Maritime Unit, Air Base and Maritime Branch, Public Works Department Malaysia

Darren, K. K. S., BEng. (Hons) MBA, Business Development/Software Manager, DHI Konsult Sdn. Bhd.

Dick, T. M., and Brebner, A. (1968). "Solid and permeable submerged breakwaters." *Proc., 11th Conf. on Coast. Engrg.*, 1141–1158.

German Federal Waterways Engineering & Research Institute, (1994). "Guidelines for testing of geotextiles in hydraulic engineering applications".

Heerten, G., (2000). "New Geotextile Developments with Mechanically bonded Non Woven Sand Containers as Soft Coastal Structures", 27th International Conference on Coastal Engineering, Sydney, Australia.

Jackson, L.A., McGrath, J. & Tomlinson, R., (1997). "Strategy for Protection of the Northern Gold Coast Beaches", Proceedings, *13th Australasian Coastal and Ocean Engineering Conference*.

Kohlhase, S., (1997). Some Aspects of the Use of Geotextiles in the Field of Coastal Engineering, Proc. of the first German-Chinese Joint Seminar - Recent Developments in Coastal Engineering, Hasenwinkel, University of Rostock, Germany.

Mei, C. C., and Black, J. L. (1969). "Scattling of surface wave by rectangular obstacles in the water of finite depth." *J. Fluid Mech.*, Cambridge, U.K., 38, 499–511.

National Coastal Erosion Study, (1984/1985), Economic Planning Unit.

Newman, J. N., (1965). "Propagation of water waves past long two-dimensional obstacles." *J. Fluid Mech.*, Cambridge, U.K., 23, 23–29.

Philip, L. F. L., (1995). “Advances in Coastal and Ocean Engineering”, World Scientific Publishing Co. Pte. Ltd., London.

Reeve, D., Chadwick, C. & Christopher, F., (2004). “Coastal Engineering: Process, Theory and Design Practice”, Spon Press, New York.

Rojanakamthorn, S., Isobe, M., and Watanabe, A. (1989). “A mathematical model of wave transformation over a submerged breakwater.” *Coast. Engrg. in Japan*, 32(2), 209–234.

Saathoff, F. & Witte, J., (1994), Use of Geotextile Containers for Stabilizing the Scour Embankments at the Eidersperrwerk, *Geosynthetics World*.

Sharp, J. J. (1981). Hydraulic Modelling, Butterworths, London, UK.

Sheng W. T., Cheng C. L., and Wen H. H. (2001). “Wave Damping Characteristics of Deeply Submerged Breakwater”, part of *Journal of Waterway, Port, Coastal, and Ocean Engineering*, Vol. 127, No. 2.

Turner, I. L., Leyden, V. M., Symonds, G., Cox, R.J., McGrath, J., Jackson, L.A., Jancar, T., Aarninkhof, S. G. J. & Elshoff, I., (2000). “Predicted and Observed Coastline Changes at the Gold Coast Artificial Reef”, *Proceedings, International Conference on Coastal Engineering, ASCE*.

U.S. Army Coastal Engineering Research Center, (1977). “Shore Protection Manual”, Department of Army Corps of Engineers.

http://unics.rrzn.uni-hannover.de/fzk/e5/projects/dune_prot_0.html

http://unics.rrzn.uni-hannover.de/fzk/e5/projects/dune_prot_0.html

<http://www.coastalmanagement.com.au/papers/>

<http://www.geotubes.com/PDF/tech%20docs/Geosystems.pdf>